The Evolution of Oceanic and Atmospheric Anomalies in the Northeast Pacific During the El Niño and La Niña Events of 1995–2001

Franklin B. Schwing [1*], Tom Murphree [2], Lynn deWitt [1], and Phaedra M. Green [1, 3]

[1] Pacific Fisheries Environmental Laboratory
NOAA NMFS SWFSC
1352 Lighthouse Avenue
Pacific Grove, CA 93950-2097

[2] Department of Meteorology
Naval Postgraduate School
Monterey, CA 93943-5114

[3] Joint Institute of Marine and Atmospheric Research
University of Hawaii
1000 Pope Road, MSB 312
Honolulu HI 96822

*Corresponding author: Franklin B. Schwing; 831-648-9034, fax: 831-648-8440, e-mail: fschwing@pfeg.noaa.gov

---

submitted to *Progress in Oceanography* 25 AUGUST 2000
revised version submitted 15 MAY 2001
special issue on "Observations of the 1997–98 El Niño along the West Coast of North America"

ABSTRACT

From late 1995 through early 2001, three major interannual climate events occurred in the tropical Pacific; the 1995-97 La Nina (LN), 1997-98 El Nino (EN), and 1998-2001 LN. We analyze atmospheric and upper oceanic anomalies in the northeast Pacific (NEP) during these events, and compare them to anomalies elsewhere in the north Pacific and tropical Pacific, and to typical EN and LN anomaly patterns. Atmospheric and oceanic anomalies varied strongly on intraseasonal and interannual scales. During the 1995-97 LN and 1997-98 EN, the NEP was dominated by negative SLP and cyclonic wind anomalies, and by upper ocean temperature and sea surface height (SSH) anomalies that were positive along the North American west coast and in the NEP thermal anomaly pool (between Hawaii, Vancouver Island, and Baja California), and negative in the central north Pacific. This atmospheric/oceanic anomaly pattern is typical of EN. An eastward shift in the atmospheric teleconnection from east Asia created EN-like anomalies in the NEP during the 1995-97 LN, well before the 1997-98 EN had begun. The persistence of negative SLP and cyclonic wind anomalies in the NEP during the 1997-98 EN intensified pre-existing upper oceanic anomalies. Atmospheric anomalies shifted eastward during late 1996–early 1998, leading to a similar onshore shift of oceanic anomalies. This produced exceptionally strong positive upper ocean temperature and SSH anomalies along the west coast during the 1997-98 EN, and explains the unusual coastal occurrence of several large pelagic warm-water fish. The growth and eastward shift of these pre-existing anomalies does not appear to have been linked to tropical Pacific EN anomalies until late 1997, when a clear atmospheric teleconnection between the two regions developed. Prior to this, remote atmospheric impacts on the NEP were primarily from east Asia. As the 1998-2001 LN developed, NEP anomalies began reversing toward the typical LN pattern. This led to predominantly negative SLP and cyclonic wind anomalies in the NEP, and upper ocean temperature and SSH anomalies that were mainly negative along the west coast and positive in the central north Pacific. The persistence of these anomalies into mid-2001, and a number of concurrent biological changes in the NEP, suggest that a decadal climate shift may have occurred in late 1998.

During 1995-2001, NEP oceanic anomalies tracked the overlying atmospheric anomalies, as indicated by the maintenance of a characteristic spatial relationship between these anomalies. In particular, wind stress curl and SSH anomalies in the NEP maintained an inverse relationship that strengthened and shifted eastward toward the west coast during late 1996–early 1998. This consistent relationship indicates that anomalous Ekman transport driven by regional atmospheric forcing was an important contributor to temperature and SSH anomalies in the NEP and CCS during the 1997-98 EN. Other studies have shown that coastal propagations originating from the tropical Pacific also may have contributed to coastal NEP anomalies during this EN. Our results

indicate that at least some of this coastal anomaly signal may have been generated by regional atmospheric forcing within the NEP.

KEYWORDS: (Atmospheric circulation; Climate; El Niño phenomena; Eastern boundary currents; Upwelling)

1. INTRODUCTION

Aside from the seasonal cycle, interannual fluctuations – associated most notably with tropical El Niño (EN) and La Niña (LN) events – are the strongest and most familiar signals of natural global variability. EN/LN events have pronounced regional effects on the physical, chemical, and biological nature of the northeast Pacific (NEP), including the California Current System (CCS). A particularly compelling series of articles in the 1960 California Cooperative Oceanic Fisheries Investigations (CalCOFI) Report describes the impacts of the 1957–58 EN on the CCS (Sette & Isaacs, 1960). This arguably was the first publication to define EN as a global event, and to associate this tropical phenomenon to changes in extratropical ecosystems. Large anomalies in the CCS have been observed in subsequent EN years as well (Enfield & Allen, 1980; Chelton & Davis, 1982; Wooster & Fluharty, 1985; Simpson, 1992; Lynn, Schwing, & Hayward, 1995; Lynn, Baumgartner, Collins, Garcia, Hayward, Hyrenbach, *et al.*, 1998). The distribution, abundance, and reproductive success of many marine populations and ecosystem structure shifted during these events (Chelton, Bernal, & McGowan, 1982; Pearcy & Schoener, 1987; Schwing & Ralston, 1995 and adjoining papers; Chavez, 1996; Lynn *et al.*, 1998; Kudela & Chavez, 2000).

Despite our long-standing awareness of EN/LN events and their remote impacts, our understanding of the processes that initiate and terminate them is incomplete. The evolution of the tropical Pacific signals of the 1997–98 EN, by many measures the strongest EN on record, was poorly predicted by forecast models (McPhaden, 1999; Barnston, Glantz, & He, 1999). The ability to understand and predict the impacts of EN events in the CCS requires a knowledge of anomalous conditions throughout the Pacific Ocean and global atmosphere, and an understanding of EN/LN processes and teleconnection mechanisms on basin and global scales. Furthermore the relative importance and timing of the mechanisms by which EN/LN influence the extratropical oceans is poorly understood. Extratropical north Pacific anomalies similar to those occurring typically during EN have been observed during non-EN periods (Emery & Hamilton, 1985; Mysak, 1986). They may even be a precursor to the development of EN events in the tropical Pacific (Namias, 1976; Emery & Hamilton, 1985; White & Tabata, 1987).

Another key issue is the degree to which anomalies in the CCS during EN/LNs – and the extratropics in general – are due to regional atmospheric forcing (which may be part of teleconnections from the tropical Pacific) versus anomalies propagating through the ocean. A number of studies indicate EN equatorial ocean signals propagate along the eastern boundary and the US west coast (Enfield & Allen, 1980; Chelton & Davis, 1982; Clarke & Van Gorder, 1994; Meyers, Melsom, Mitchum, & O'Brien, 1998; Strub & James, 2001). Other studies suggest low-frequency coastal-trapped wave energy cannot propagate effectively into the CCS (Baumgartner & Christensen, 1985; Mysak, 1986; McAlpin, 1995; Clarke & Lebedev, 1999). Still others indicate the EN signature in the CCS is due mostly to local and regional Ekman processes (Emery & Hamilton, 1985; Mysak, 1986; Simpson, 1992; Murphree & Reynolds, 1995; Miller, White, & Cayan, 1997).

In this paper we describe the temporal evolution of the coastal environment within the central CCS, and the regional (NEP) and large-scale atmospheric and oceanic fields as they evolved through the EN and LN events of 1995–2001. We track the development of three major events; the 1995–97 LN, the 1997–98 EN, and the LN that began in 1998 and continued into 2001. Large atmospheric and oceanic anomalies occurred in the CCS and throughout the north Pacific during these events. The differences between them and typical EN/LN anomalies are described. Finally, we discuss some mechanisms that appear to have contributed to these unusual conditions.

The focus of this study is on anomalies in the CCS, and in the NEP generally, during the 1997–98 EN event. However NEP anomalies that were established a priori were critical to the development of some dramatic anomalies during this event. Conditions in the north Pacific during the 1995–97 LN were unusual in the context of a typical LN state. They set the stage for alterations in the extratropical ocean associated with the development of a very strong EN in early 1997, and may have contributed to the rapid growth of this event. The unusually rapid and large transition from EN to LN in 1998 also merits discussion, particularly because of the dramatic biological shifts in the CCS associated with it (Schwing, Moore, Ralston, & Sakuma, 2000).

We use the following geographical definitions to highlight regional differences in oceanic and atmospheric fields during EN and LN events. The *tropical Pacific* is the region between southeast Asia and the Americas, from 10°S to 10°N. This region is composed of: the *western tropical Pacific*, which lies east of the dateline; the *central tropical Pacific*, between the dateline and 140°W; and the *eastern tropical Pacific*, east of 140°W. The *central north Pacific* (CNP) is from 20°N to 50°N, and 165°E to 155°W. The *NEP* is north of 20°N and east of 155°W, roughly north and east of Hawaii. The *CCS* is between about 25°N and 45°N, and within about 1000 km of the North American west coast.

We also focus on three spatial scales to describe the processes and mechanisms that may influence oceanic variability in the NEP. (1) *Local processes* occur over scales of tens of kilometers. Important examples in the NEP are air-sea heat fluxes, turbulent mixing, and coastal upwelling and downwelling. Vertical fluxes of mass, momentum, and energy tend to be especially important for local processes. (2) *Regional processes* occur over scales of hundreds of kilometers. These include processes related to wind stress curl (e.g., open-ocean Ekman pumping). (3) *Remote processes* operate over thousands of kilometers. Important examples for this study include atmospheric teleconnections and low-frequency internal wave propagations through the atmosphere and ocean. All of these processes operate on a wide range of temporal scales. However smaller (larger) spatial-scale processes tend to have shorter (longer) temporal scales. The principal time scales of focus here are intraseasonal (1–4 months) and interannual (>12 months) which, as will be seen, are the important scales of variability in the CCS during EN/LN events.

2. DATA AND METHODS

2.1. COASTAL TIME SERIES OFF CENTRAL CALIFORNIA

Time series representing conditions in the CCS were created from two sources. Wind and sea surface temperature (SST) observations off central California (35–39°N) were obtained from NOAA National Data Buoy Center (NDBC) buoys (http://www.ndbc.noaa.gov/). Dorman & Winant (1995) have shown that winds in this region are highly coherent. To cover frequent data gaps in recent years, composite daily time series of alongshore wind and SST were created from all available buoy observations in this region (Table 1). Coastal sea level data were obtained from the University of Hawaii Sea Level Center (http://uhslc.soest.hawaii.edu/). The sea level series used here is a composite of daily detided data from Crescent City and Fort Point (San Francisco), California. Sea level data were not adjusted for atmospheric pressure effects. Daily climatologies of these coastal time series were determined by an annual and semiannual fit to each long-term (1981–99) composite series. These were subtracted from the series to produce daily anomalies. The daily series have been 30-day smoothed to remove short-term (synoptic) variability. The wind series was 90-day smoothed to highlight interannual variability.

2.2. PACIFIC ATMOSPHERIC AND OCEANIC ANOMALY FIELDS

Large-scale anomalies are summarized in maps of NCEP reanalysis fields (Kalnay *et al.*, 1996) from the NOAA–CIRES Climate Diagnostics Center (http://www.cdc.noaa.gov/). These maps illustrate the evolution of EN and LN events that affected the NEP. The reanalysis fields described here are monthly gridded (roughly 2° x 2°) anomaly fields of SST, SLP, 850-hPa wind

velocity, and 200-hPa geopotential height. The 850-hPa winds describe the low-level (surface to lower tropospheric) wind field. The 200-hPa heights are used to determine upper-level (upper tropospheric) atmospheric circulations and identify atmospheric teleconnections. The base period for computing the NCEP reanalysis field anomalies is 1968–96.

Subsurface ocean temperature anomaly maps are based on the Global Temperature-Salinity Profile Program (GTSPP) data base (http://www.nodc.noaa.gov/GTSPP/gtspp-home.html). Temperature data were monthly averaged on a 1° spatial grid and interpolated vertically at 19 standard depths, including the 100-m level shown in this paper. Anomalies were computed by subtracting the 1° monthly climatologies (base period 1945–96) of the World Ocean Database 1998 (Levitus, Boyer, Conkright, O' Brien, Antonov, Stephens, *et al.*, 1998) from the gridded observations. Because subsurface data are sparse, the anomalies were averaged into 5° x 5° spatial boxes for mapping. The median number of observations in the boxes on these maps is about five. White areas denote no data for the period shown.

Sea surface height (SSH) anomalies were provided by the NOAA Laboratory for Satellite Altimetry (http://ibis.grdl.noaa.gov/SAT/), based on data from the joint NASA/CNES TOPEX/Poseidon satellite altimeter. SSH deviations were averaged by month in 4° longitude x 1° latitude cells to construct regular grids of SSH deviation relative to 1993–1995. Their anomalies were computed by removing the annual and semiannual harmonics. The anomaly maps are composites from a series of months that represent the patterns characteristic of various time periods or climate events, as described in detail below and in Table 2.

The comparison of climatologies and anomalies involves a variety of data sets and types with different base periods. Our analysis of this issue indicates the results described here are not significantly altered by changing the base period. The magnitude of anomalies during EN/LN is quite large, and the patterns are qualitatively the same regardless of the climatological period. Beyond the data gridding described above, anomaly fields were not smoothed for plotting.

2.3. DEFINING EL NINO AND LA NINA PERIODS

A number of indices have been developed to quantify the magnitude and timing of climate events, including EN/LN. We use the Multivariate ENSO Index or MEI (Wolter & Timlin, 1998) as an index of EN/LN conditions in the tropical Pacific, and to define the characteristic periods of these events since 1995 (Table 2). The MEI is based on six well-correlated observed variables in the tropical Pacific: SST, atmospheric sea level pressure (SLP), zonal and meridional surface winds, surface air temperature, and total cloudiness. Details on the computation of the MEI are available at: http://www.cdc.noaa.gov/~kew/MEI/mei.html.

Figure 1 shows the evolution of the MEI since 1995. Positive (Negative) MEI values represent EN (LN) periods and identify three recent events; the 1995–97 LN, the 1997–98 EN, and the 1998–2001 LN. These events were separated by relatively rapid transitions, which are represented by sharp changes in the magnitude and sign of the MEI. The sequence of these events is given in Table 2. The time periods of EN/LN events based on other criteria (e.g., Trenberth, 1997) are very similar to those based on the MEI. Figure 2 compares these recent events to past strong events. EN and LN typically develop and decay in the boreal spring. However the 1997–98 EN and 1998–2001 LN developed at a rate unprecedented in recent history.

On interannual time scales, SLP variations over the NEP are out of phase with those over the western tropical Pacific; this led to the development of the extratropical Northern Oscillation Index or NOIx (Schwing, Murphree, & Green, 2001), a climate index similar to its tropical equivalent, the Southern Oscillation Index. The NOIx is computed from the difference between SLP anomalies of the North Pacific High (35°N, 135°W) and Darwin, Australia (10°S, 130°E). It is primarily an index of the north Pacific Hadley–Walker circulation, including trade winds and subtropical jet streams, induced by a variety of climate phenomena. It is significantly correlated with interannual variability in a number of atmospheric and oceanic fields in the NEP (Schwing *et al.*, 2001). The NOIx is available at: http://www.pfeg.noaa.gov.

The NOIx since 1995 is shown in Figure 1 along with the MEI. The NOIx is generally negative (positive) during EN (LN), and negatively correlated with the MEI. The close correspondence between these two independent climate indices shows that the atmosphere over the NEP fluctuates with, and thus is likely coupled with, atmospheric and oceanic conditions in the tropical Pacific. The evolution of recent EN/LN, as defined by the MEI, NOIx, and other indices, is apparent in a number of atmospheric and oceanic fields throughout the Pacific. As we show in section 3, the 1997–98 EN and 1998–2001 LN events were characterized by distinct atmospheric and oceanic anomaly patterns that imply a connection between the tropical and extratropical Pacific.

3. RESULTS

3.1. TYPICAL EL NIÑO AND LA NIÑA ANOMALIES IN THE PACIFIC

The major anomalies that typically develop in the Pacific during EN (LN) events are described in Figure 3 (Figure 4) by composite anomaly patterns for SST, 100-m ocean temperature, 200-hPa geopotential height, SLP, and 850-hPa wind during November–February, based on ten moderately to very strong EN (LN) events during 1960-1995 (Table 3). Boreal winter anomalies are shown because this is when EN/LN events are typically in their mature phase.

SST anomalies (SSTAs) in the north Pacific during EN (LN) are: (1) cool (warm) in the western tropical Pacific; (2) warm (cool) in the central and eastern tropical Pacific; (3) cool (warm) in the CNP; and (4) warm (cool) in the NEP (Figs. 3a, 4a). Stronger SSTAs in the eastern tropical Pacific and NEP are separated by weaker SSTAs off southern Mexico. Pacific SSTAs are approximately symmetric about the equator. Subsurface temperature anomaly patterns (Figs. 3b, 4b) are similar to the SSTAs, with a few modifications. Western tropical Pacific subsurface anomalies are more extreme, reflecting shoaling (deepening) of the thermocline in the western Pacific warm pool during EN (LN). Subsurface anomalies during the mature phase of EN give a stronger impression than SSTAs of an equatorial connection to the North American coast.

In the EN (LN) composite, tropical Pacific low-level wind anomalies are eastward (westward), indicating weak (strong) trade winds, and strong wind convergence (divergence) in the central and eastern tropical Pacific (Figs. 3d, 4d; cf. Rassmusson & Carpenter, 1982). The eastward (westward) zonal wind anomalies along the equator lead to anomalous equatorial downwelling and eastward (westward) currents which contribute to positive (negative) SSTA anomalies in the central and eastern tropical Pacific in the EN (LN) composites (Figs. 3a,b, 4a,b; Philander 1990; McPhaden, 1999).

The trade wind anomalies also are part of coherent extratropical wind anomalies that emanate out of high pressure systems in the eastern regions of the north and south Pacific. These atmospheric anomalies are roughly symmetric about the equator. For example, Figure 3d (4d) shows that large cyclonic (anticyclonic) surface wind anomalies during EN (LN) in the NEP and the southeastern Pacific (centered near 35°S, 120°W) are associated with negative (positive) SLPA centers and weaker (enhanced) trade winds. A common tropical Pacific forcing source may initiate this symmetry, perhaps via variations of the north and south Pacific branches of the Hadley–Walker circulation (cf. Bjerknes, 1969; Rassmusson & Carpenter, 1982, Schwing *et al.*, 2001).

Over the CNP and NEP, negative (positive) SLPAs correspond to a stronger (weaker) Aleutian Low and weaker (stronger) North Pacific High during EN (LN). These SLPAs result in anomalous forcing of the upper ocean with, for example, cyclonic (counter-clockwise in the northern hemisphere) wind stress anomalies over the NEP during EN, including poleward (downwelling-favorable) winds along the west coast of North America (Fig. 3d), and the opposite forcing anomalies in LN (Fig. 4d).

During EN/LN, SLPAs and SSTAs in the CNP and NEP have a "characteristic spatial relationship" (Figs. 3a,d and 4a,d). Specifically, the center of the negative (positive) SLPA in the CNP and NEP tends to be bounded to the north and east by positive (negative) SSTAs, and to the south and west by negative (positive) SSTAs. Similar spatial relationships between SLPAs and

SSTAs were found during the different phases of the EN and LN events of 1995–2001 (see section 3.3). Namias, Yuan, & Cayan (1988) found a similar pattern and relationship between monthly 700-mb height and SST anomalies for 1947–86. Our analyses of the evolution of recent NEP anomalies emphasize the role of SLPAs in these regions, and their associated low-level wind anomalies.

The mechanisms by which extratropical oceanic anomalies are generated by regional wind anomalies – including Ekman processes, geostrophic advection, surface heat fluxes, and mixing – have been addressed in a number of studies (e.g., Cayan, 1992; Miller, Cayan, Barnett, Graham, & Oberhuber, 1994; Miller & Schneider, 2000), but the relative importance of each has not yet been well determined. All may contribute to the characteristic SLPA-SSTA relationships shown in Figures 3 and 4. In section 3.4, we discuss the possible importance of Ekman processes in explaining a number of the NEP upper oceanic anomalies that occurred during 1995–2001.

Extratropical atmospheric anomalies are equivalent barotropic (i.e., the anomalies are qualitatively similar from the upper troposphere to the surface) (Figs. 3c,d and 4c,d). For example, in the EN (LN) composites, the 200-hPa and SLP anomaly fields are positive (negative) over the western subtropical north Pacific, negative (positive) over most of the CNP and NEP, and positive (negative) over North America (Figs. 3c,d, 4c,d).

Two main mechanisms have been proposed for the remote forcing of oceanic anomalies in the NEP during tropical EN/LN: (1) atmospheric teleconnections involving wave trains from the western and central tropical Pacific (Horel & Wallace, 1981; Emery & Hamilton, 1985; Mysak, 1986; Simpson, 1992; Murphree & Reynolds, 1995); and (2) oceanic poleward propagating coastal-trapped waves (Enfield & Allen, 1980; Chelton & Davis, 1982; Clarke & Van Gorder, 1994; Meyers *et al*., 1998), principally baroclinic Kelvin waves.

Evidence for atmospheric teleconnections into the NEP during EN/LN is clear in the composite geopotential height anomalies (Figs. 3c, 4c). These teleconnections are represented by patterns of alternating positive (H) and negative (L) 200-hPa height anomalies, which represent anomalous wave trains that are typical in November-February during EN/LN. For example, during EN an anomalous wave train originating in the central tropical Pacific is revealed by a positive height anomaly centered near Hawaii, a negative over the CNP–NEP, a positive over Canada, and a negative near Iceland (Fig. 3c). A comparable but oppositely signed anomalous wave train pattern occurs during LN (Fig. 4c). These patterns are similar to the Pacific/North American (PNA) pattern, a familiar example of an anomalous wave train associated with positive (negative) tropospheric heating anomalies in the central and eastern tropical Pacific during EN (LN) (Wallace and Gutzler, 1980; Horel & Wallace, 1981; Peixoto & Oort, 1992).

Figures 3c and 4c also show anomalous wave trains emanating from east Asia and arching over the NEP and North America. For example, during LN (Fig. 4c) an anomalous wave train is indicated by a positive height anomaly over eastern China, a negative southeast of Japan, a positive over the CNP–NEP, a negative over Canada, and a positive near Iceland. Similar anomalous wave trains have been identified in several previous studies, and are associated with tropospheric heating anomalies in the southeast Asia–western tropical Pacific region (e.g., Nitta, 1987; Ford, 2000; Murphree, Schwing, & deWitt, 2001). An analogous but oppositely signed anomaly pattern occurs during EN (Fig. 3c). The arrows in Figures 3c and 4c indicate the anomalous wave trains originating near Hawaii and near east Asia intersect and interfere constructively over the NEP, North America, and the north Atlantic. In these extratropical regions, the impacts of EN/LN due to atmospheric teleconnections tend to originate from both the central tropical Pacific and east Asia. These anomalous wave trains and their role in the origin of surface anomalies in the NEP during 1995-2001 are discussed in section 3.5.

In analyzing EN and LN events and their impacts, especially in the NEP, three fundamental points must be considered. First, EN/LN are tropical phenomena but have extratropical impacts. Second, anomalies that appear to be caused by EN/LN can be produced by other phenomena and processes. Third, because of the slow response of the ocean (principally due to its thermal and mechanical inertia) to atmospheric change, the oceanic impacts of EN/LN events can linger long after the atmospheric processes that caused them have dissipated. Attribution of extratropical anomalies to EN/LN is a complex and difficult issue. A clear *mechanistic* connection to the tropical Pacific should be shown before ascribing extratropical anomalies to tropical EN or LN events.

3.2. COASTAL CONDITIONS OFF CENTRAL CALIFORNIA, 1995–99

The time series in Figure 5 describe the temporal evolution of anomalous wind forcing over the central CCS (35–39°N)1995–99, and its relationship to coastal SST and coastal sea level (CSL) anomalies. They reflect extremes that may have been linked to regional-, basin-, and global-scale anomalies. These seasonally adjusted coastal series varied on two primary scales; interannual (>12 months) and intraseasonal (1–4 months).

On interannual scales, central California coastal wind anomalies (Fig. 5a) were generally positive (downwelling- or weaker upwelling-favorable) during the 1997–98 EN. SST and CSL anomalies (Fig. 5b,c) also were positive, and rose rapidly as EN reached maturity. Between April and July 1997, a subsurface intrusion of anomalously warm saline water appeared in the Southern California Bight in association with a very strong California Undercurrent (Lynn & Bograd, 2001). Warm saline poleward coastal flow was observed in late July off central California (Collins, Castro,

Asanuma, Rago, Han, Durazo, *et al.*, 2001) and in September off southern California (Lynn & Bograd, 2001) and Oregon (Huyer, Smith, & Fleischbein, 2001). This broad coastal anomaly may have contributed to the increasing SST and CSL shown in Figure 5. Central California SST anomalies were greatest in autumn 1997, as much as 6°C above the seasonal mean at some locations. CSL anomalies continued to rise in late 1997 and early 1998 after SST anomalies began falling, and peaked in February 1998. By April 1998 SST and CSL had declined to normal levels.

In contrast to the coastal anomalies during EN, the 1995–97 LN featured predominantly southward (upwelling-favorable) wind anomalies in the CCS (Fig. 5a), and corresponding negative SST and CSL anomalies (Fig. 5b,c). Southward coastal wind anomalies dominated again in the 1998–99 LN, coinciding with a dramatic shift in spring 1998 from a strong poleward countercurrent to a strong southward flow (Hayward, Baumgartner, Checkley, Durazo, Gaxiola-Castro, Hyrenbach, *et al.*, 1999). SST and CSL anomalies became negative in late 1998, and declined even further in April–May 1999 off much of California and Baja California. SST anomalies were as much as 3–4°C below normal during the 1999 upwelling season. CSL was unseasonably low during 1999.

During these LN and EN events, anomalous intraseasonal southward (northward) wind events, corresponding with negative (positive) SST and CSL anomalies, tended to mask interannual variability. Strong northward wind anomalies (Fig. 5a) in February 1996 and December 1996–January 1997, during the 1995–97 LN, led to increased positive SST and CSL anomalies (Fig. 5b,c). Similar winter events occurred during the 1994–95 EN in January and March 1995, and the 1997–98 EN in November 1997 and February 1998. These northward wind anomalies occurred during periods of intense winter storm activity.

Following the storms and downwelling of January 1997, a very strong intraseasonal upwelling (negative wind anomaly) event in February, coinciding with the demise of the 1995–97 LN, lowered SST and CSL. Downwelling wind anomalies preceded warming events during EN in May and August 1997. These events were apparent as positive sea level anomalies, which Strub & James (2001) interpreted as the extratropical expression of equatorial Kelvin waves. They were followed by anomalously strong upwelling winds that temporarily lowered SST and CSL anomalies off central California. Rising (Declining) surface salinity (not shown) accompanied most of the intraseasonal upwelling (downwelling) wind anomaly events shown in Figure 5. The May wind event, at the onset of the 1997–98 EN, helped initiate positive SST and CSL anomalies that remained for several months. It was part of a large-scale extratropical anomaly that may have contributed significantly to the rapid intensification of tropical EN conditions (Murphree &

Schwing, 2001). Downwelling wind anomalies accompanied the two highest CSL events in November 1997 and February 1998.

A series of strong upwelling wind events during late 1998 and the first half of 1999, coinciding with the development of LN, contributed to dramatic cooling and large CSL declines. Two particularly strong upwelling events in early May and June 1999 led to seasonal SSTs and CSLs that were among the lowest in over 50 years (Schwing & Moore, 2000; Schwing *et al.*, 2000). Thus, local wind anomalies on interannual and intraseasonal scales appear to have contributed strongly to major variations of CCS SST and CSL during recent EN and LN events.

3.3. LARGE-SCALE OCEANIC AND ATMOSPHERIC CLIMATE PATTERNS

We now examine the large-scale context in which these conditions in the CCS evolved. In the following sections, the basin- to global-scale anomalies that influenced the NEP are described for the major phases of EN and LN during 1995–2001 (Table 2), based on the MEI and NOIx (Fig. 1). We highlight the anomaly patterns in the NEP and CCS, and their possible connections to larger scale anomalies.

3.3.1. The 1995–97 La Niña: September 1995 – February 1997

Weak to moderate LN conditions appeared in the tropical Pacific in about September 1995 and continued through February 1997 (Table 2, Figs. 1, 2). The north Pacific during this time was dominated by a horseshoe-shaped region of positive SSTAs surrounding negative SSTAs in the central and western basin (Fig. 6a). From the NEP, positive SSTAs extended zonally across the subarctic north Pacific, and southwestward into the western tropical Pacific, approximately along the main path of the trade winds. An area of strong positive SSTAs was centered in the closed (eastern) end of the horseshoe, between Hawaii, Vancouver Island, and Baja California. This feature, which we term the NEP thermal anomaly pool, persisted well into the 1997–98 EN, and appears to have been important in the unusual development and strength of oceanic anomalies in the NEP during that event. The coastal Gulf of Alaska was cooler than normal. Pacific SSTAs were roughly symmetric about the equator, with positive SSTAs extending from the mid-latitude southeast Pacific northwestward to the western tropical Pacific.

Subsurface temperature anomalies (Fig. 6b) during the 1995–97 LN displayed a pattern very similar to the SSTAs. They were positive in the western tropical Pacific, in much of the NEP, and across the subarctic north Pacific. Subsurface temperature anomalies were negative in the eastern tropical Pacific and CNP. High (Low) SSH anomalies (SSHAs) in the extratropical north and south Pacific (Fig. 6c) corresponded roughly with warm (cool) anomalies.

The overall upper oceanic anomaly pattern in the north and south Pacific resembled the typical LN state (cf. Figs. 4, 6). However the 1995–97 LN pattern in the north Pacific was relocated about 25° longitude east of the composite LN pattern. For example, a band of positive SSTAs extending between the western tropical Pacific and the extratropical north Pacific was shifted significantly further east in 1995–97 (cf. Figs. 4a, 6a). This led to positive temperature anomalies in most of the NEP, where SSTAs during LN events typically are negative. Similar eastward relocations of the typical SSTA patterns occurred into the CNP and the Gulf of Alaska.

Anomalously cyclonic large-scale winds over much of the north Pacific contributed to unusually weak north Pacific trade winds (Fig. 6d), plus unusually strong onshore flow and heavy precipitation in the Pacific Northwest during the winters of 1995–96 and 1996–97. South Pacific wind anomalies were similar spatially to the composite LN, with unseasonably strong trade winds emanating out of the southeast Pacific and connecting to anomalously westward equatorial winds west of the dateline (cf. Fig. 4d, 6d).

The eastward shift in north Pacific oceanic anomaly patterns, compared to typical LN events, corresponds with a similar relocation in atmospheric forcing. In particular, the negative SLPA centered southeast of Japan in the composite LN was shifted eastward into the CNP, and the positive SLPA centered typically in the CNP was located further to the east near North America (cf. Figs. 4d, 6d). Despite these eastward shifts, the SSTAs surrounding the negative SLPA in the CNP and NEP showed the characteristic spatial relationship described in section 3.1 (cf. Figs. 3, 4, 6).

North Pacific SSTAs during the 1995–97 LN were similar visually to the positive SSTAs that are typical of the mature phase of EN events (cf. Figs. 3a, 6a). Positive SSTAs in spring–summer 1997 may be incorrectly characterized as the early impacts of the 1997–98 EN event, when in fact they were the lingering effects of the unusual 1995–97 LN. The persistence of these SSTAs was related to a continuation during the 1997-98 EN of the anomalously cyclonic low-level winds that dominated the CNP and NEP during the 1995-97 LN, as described section 3.3.2. Possible mechanisms linking SLP and low-level wind anomalies to the SSTAs during the 1995–97 LN will be discussed in section 3.4. We also will show evidence that the eastward shift of surface atmospheric anomalies was related to an eastward relocation of anomalous wave trains and teleconnections that affected the north Pacific during this event (section 3.5).

3.3.2. The 1997–98 El Niño

3.3.2.1. Rapid Intensification: March–June 1997

In late 1996 and early 1997, anomalous eastward wind bursts in the western equatorial Pacific (Fig. 7a) helped initiate a transition toward EN conditions (Chavez, Strutton, & McPhaden,

1998; McPhaden, 1999; Murphree and Schwing, 2001; cf. Rassmusson & Carpenter, 1982). This led to the swift development and eastward expansion of positive upper ocean temperature anomalies (Figs. 7b, 8a,b), an anomalously deep thermocline (Fig. 7c), and strong positive SSHAs (Fig. 8c) in the central and eastern equatorial Pacific. This EN developed very rapidly during boreal spring 1997 (Figs. 1, 2). By July 1997 atmospheric and oceanic anomalies in the tropical Pacific were unusually intense, especially for so early in the calendar year (Figs. 2, 8).

South Pacific oceanic anomalies shifted to a typical EN pattern during March–May 1997 (cf. Figs. 3a,b, 8a,b). In the extratropical north Pacific, upper ocean temperature and SSH anomalies during spring 1997 remained similar to those during most of the 1995–97 LN, but were stronger and centered further to the east (cf. Figs. 6a-c, 8a-c). In particular, positive oceanic anomalies were much stronger in the NEP, and more extensive along the west coast. By early June 1997, NEP SSTAs ranged from +0.5°C to more than +4.0°C.

Spring 1997 atmospheric anomalies are reflected in the North Pacific High. Normally during the boreal spring, the High migrates to the northwest from its winter position off Baja California, and expands and strengthens to the west. This development was unusually weak in 1997, leading to negative SLP and cyclonic wind anomalies over much of the CNP and NEP (Fig. 8d). The effects of these atmospheric anomalies were very pronounced in the CCS, where alongshore wind, SST, and CSL anomalies became positive during spring 1997 (Fig. 5). Changes in the CCS were especially rapid during May 1997, when the CNP and NEP atmospheric anomalies summarized in Fig. 8d were even more pronounced and further to the northeast.

Like SSTAs, SLP and wind anomalies in the CNP and NEP were similar in winter 1996–97 and spring 1997, with spring anomalies stronger and occurring further to the northeast (cf. Figs. 6d, 8d). SSTAs were positive (negative) to the east and north (west and south) of the negative SLPA in the CNP and NEP in both seasons (cf. Figs. 6a,d, 8a,d), the characteristic spatial relationship described for EN in section 3.1. This correspondence suggests that the intensification and shifting of NEP oceanic anomalies in the early phase of the 1997–98 EN (i.e., spring 1997) was due to similar changes in the overlying atmospheric anomalies.

By spring 1997, the highest temperature and SSH anomalies were closer to the North American coast than during the preceding winter, but were still not part of a coastally confined feature (cf. Figs. 6a-c, 8a-c). The rapid development of coastal oceanic anomalies was consistent with the evolution of NEP atmospheric anomalies. There were no clear indications that the intensification of oceanic anomalies in the NEP thermal anomaly pool was related to those in the eastern tropical Pacific (Fig. 8a-c). These observations suggest that major warming patterns over much of the NEP and CCS during spring 1997 were not linked directly by oceanic teleconnection

to the simultaneous warming in the central and eastern tropical Pacific. Instead, the warming in the NEP appears to have been largely due to pre-existing positive temperature anomalies and changes in the overlying regional atmospheric forcing (see section 3.4 for more detail).

3.3.3.2. Mature El Niño: July 1997 – March 1998

By August–September 1997, the 1997–98 EN had reached a very intense initial peak (Figs. 1, 2). Negative upper ocean temperature and SSH anomalies had intensified in the western tropical Pacific (Fig. 9a-c). In the central and eastern tropical Pacific, this was a period of very warm SSTs and an anomalously deep thermocline, related to strongly eastward low-level wind anomalies that were convergent in the eastern tropical Pacific (Fig. 7). Strongly positive SSTAs extended along the equator east from the dateline, and poleward from the equator to northern Chile and Nicaragua (Fig. 9a).

Ocean temperature and SSH anomalies were positive along most of the North American west coast (Fig. 9a-c). Positive (Negative) SSTAs in the NEP thermal anomaly pool (CNP) were centered further to the northeast than during the preceding spring. Surveys off Oregon found a similar onshore shift in the warmest surface anomalies from July to September (Huyer *et al*., 2001).

The development of positive SSTAs in the NEP thermal anomaly pool and exceptionally warm coastal temperatures had important ecological implications. Pearcy (2001) observed that the exotic marine species sighted in the CCS in the early phase of the 1997–98 EN were very different from those occurring during the 1982–83 EN. The 1997–98 assemblage was comprised of large pelagic fish; warm-water oceanic species that are strong migrators. The positive thermal anomaly pool represented an eastward expansion of the normal habitat of these fish, extending their range into coastal waters. The expatriots reported later in 1998 were coastal demersal animals that probably relied on enhanced coastal currents for northward transport (Pearcy, 2001). These are similar to the types of exotic animals seen in the 1982–83 event (cf., Simpson, 1992). Subsurface temperature and SSH anomaly patterns were similar to SSTAs, but positive anomalies extended poleward from the equator to the Gulf of California (Fig. 9b,c). Subsurface anomalies during boreal summer 1997 are consistent with a continuous coastal oceanic teleconnection from the eastern tropical Pacific into the NEP, but do not resolve it clearly.

Negative SLP and cyclonic wind anomalies remained over much of the northern NEP during July-September 1997, as they had during the preceding winter and spring. However these anomalies continued their apparent eastward migration since the previous winter (cf. Figs. 6d, 8d, 9d). The characteristic spatial relationship between the SLPA and surrounding SSTAs seen in the 1995–97 LN and spring 1997 remained intact (see section 3.1; cf. panels a and d of Figs. 3, 6, 8).

In particular, cyclonic wind anomalies over the NEP may have caused anomalous onshore Ekman transports, coastal downwelling, and positive coastal SSHAs (Figs. 5b,c, 9a-c). The latter may have led to positive geostrophic temperature advection, reinforcing anomalously warm SSTs along the US west coast. This was occurring at a time when west coast SSHAs suggested an oceanic teleconnection with the eastern tropical Pacific (Strub & James, 2001).

In early 1998, EN reached a second peak in intensity (Figs. 1, 2). Pacific atmospheric and upper oceanic anomaly fields closely resembled the composite mature EN patterns (cf. Figs. 3, 10). The equatorial Pacific had eastward wind anomalies that extended from the dateline to South America (Fig. 7a), and an unusually shallow (deep) thermocline in the western (eastern) equatorial Pacific (Fig. 7c). Positive upper oceanic anomalies were weaker in the NEP thermal anomaly pool (Fig. 10a-c), but stronger in the CCS and more closely confined to the coast (Figs. 5b, 10a-c). Negative oceanic anomalies in the CNP were more coherent spatially and centered further to the east than during July–September 1997 (cf. Figs. 9a-c, 10a-c). In the Gulf of Alaska, positive ocean temperature anomalies were weaker, and SSH anomalies were more negative (Figs. 5c, 10c).

The continuing intensification and eastward shift of upper oceanic anomalies in the north Pacific was consistent with the corresponding changes in atmospheric SLP and wind anomalies (Fig. 10d). In particular, from boreal summer 1997 to winter 1997–98, negative SLP and cyclonic wind anomalies in the CNP and NEP strengthened and expanded to the east and south over western North America (cf. Figs. 9d, 10d). These anomalies represented a deeper Aleutian Low that extended further to the southeast than during the typical winter (cf. Hartmann, 1994). The corresponding winter storm activity was unusually intense, with heavy precipitation along the west coast of North America, especially during February 1998. Anomalies during winter 1997–98 also were shifted eastward with respect to the composite EN anomalies (cf. Figs. 3, 10). For example, the negative SLPA centered over the Bering Sea in the EN composite was just south of the Gulf of Alaska during winter 1997–98 (cf. Figs. 3d, 10d). This is consistent with the CNP and NEP SSTAs being more closely confined to the west coast during winter 1997–98 than in the composite (cf. Figs. 3a, 10a). As in the preceding twelve months, atmospheric anomalies in the CNP and NEP appear to have been closely linked with the position of the underlying oceanic anomalies during the mature phase of the 1997–98 EN.

3.3.2.3. Transition toward La Niña: April – July 1998

Pacific upper ocean temperature anomalies during March-April 1998 were still characteristic of EN conditions. Positive anomalies (+2–4°C) extended along the equator from the dateline to South America (Fig. 7b). North and South American coastal SSTs remained unseasonably warm

(+1–3 °C anomalies) while negative (-1–3°C) anomalies persisted in the CNP and central south Pacific (Hayward *et al*., 1999).

However the intensification of anomalously cool subsurface temperatures in the equatorial Pacific in boreal spring 1998 (Fig. 7c) indicated a continuing transition away from EN conditions that began in late 1997. In May–June 1998, westward wind and negative SST anomalies were returning to the central and eastern tropical Pacific (Fig. 7a,b). Two distinct regions of negative SST and SSH anomalies developed in spring 1998; in the western and central tropical Pacific and in the NEP thermal anomaly pool. By July, the transition toward LN conditions was well established, with positive (negative) upper ocean temperature and SSH anomalies developing in the far western (central and eastern) tropical Pacific (Figs. 7b,c, 11a-c). SLP and trade wind anomalies were positive in both the extratropical north and south Pacific (Fig. 11d), a precursor to the developing LN (Rasmusson and Carpenter, 1982; Murphree & Schwing, 2001).

An unseasonably strong North Pacific High developed and persisted in summer 1998, and SLPAs in the NEP and CNP became positive (Fig. 11). Along the North American west coast , positive SLPAs corresponded to negative low-level wind anomalies that favored greater coastal upwelling and a trend toward negative coastal SST and SSH anomalies (Fig. 5a-c; cf. Figs. 10c, 11c). The underlying oceanic anomaly fields also changed, in a manner consistent with the characteristic spatial relationship between atmospheric and oceanic anomalies (see section 3.1).

3.3.3. The 1998–2001 La Niña

3.3.3.1. Rapid Intensification: August – October 1998

The MEI and NOIx changed signs in August 1998, indicating a shift toward LN conditions (Fig. 1). Equatorial zonal wind anomalies were divergent over the central tropical Pacific (Figs. 7a, 11d), cf. convergent wind anomalies in the 1997–98 EN. This contributed to decreases in upper ocean temperature, thermocline depth, and SSH in the central and eastern tropical Pacific (Figs. 7c, 11a-c). A shift to strong equatorward winds in early boreal autumn helped produce lower than normal SSTs and SSHs in the CCS (Fig. 5a-c). However subsurface temperatures remained above normal, indicating a gradually shoaling but anomalously deep thermocline along the North American west coast (cf. Figs. 10b, 11b, 12b).

3.3.3.2. Mature La Niña: November 1998 – early 2001

By boreal winter 1998–99, atmospheric and oceanic anomalies indicated a mature LN had developed in the tropical Pacific (Figs. 1, 2), with impacts that extended well into the extratropical north and south Pacific (Fig. 12). SSTs more than 2°C below normal occurred in much of the

central tropical Pacific (Figs. 7b, 12a). Divergent low-level winds in the tropical Pacific west (east) of the dateline (Figs. 7a, 12d) led to an unusually deep (shallow) thermocline and positive (negative) subsurface temperature anomalies (cf. Figs. 7c, 12b).

Negative SSTAs stretched roughly along the axis of the trade winds from the central tropical Pacific to California and northern Mexico, and into the NEP thermal anomaly pool (Fig. 12a), although the underlying temperature anomalies were positive (Fig. 12b). SST and SSH anomalies in most of the CNP and NEP were negative (Fig. 12a,c). However positive temperature and SSH anomalies had intensified and expanded over a broad region from the western subtropical Pacific into the CNP north of Hawaii.

SLPAs over most of the CNP and NEP were positive, with anomalously strong trade winds extending from the west coast of North America into the western tropical Pacific (Fig. 12d). The characteristic spatial relationship between SLPAs and SSTAs was again present. Despite strong upwelling-favorable wind anomalies in the CCS, positive coastal subsurface temperature anomalies persisted but were diminishing. SLP and wind anomalies in the south Pacific were similar to those in the north Pacific, with a strong South Pacific High and trade winds.

Upper ocean temperature anomalies in most of the north Pacific had intensified further by May–June 1999 (Figs. 5b,13a,b), particularly in the CCS where SSTs were as much as 3–4°C below normal. In much of the CNP and NEP, SSTAs were roughly opposite those during the 1997–98 EN (cf. Figs. 8a, 9a, 10a, 13a). Positive subsurface temperature anomalies were seen along the west coast and in the NEP thermal anomaly pool, with negative anomalies to the west (cf. Figs. 10b, 13b). This anomaly pattern can be traced back prior to the 1997–98 EN, when these features were qualitatively similar but located further west (cf. panel b of Figs. 6, 8-13). The broad zonal region of positive upper ocean temperatures and SSHAs centered at about 30°N in the western north Pacific continued its eastward expansion into the NEP (cf. Figs. 12a-c, 13a-c). In most of the north and south Pacific, SSHAs were positive (negative) where SSTAs were positive (negative) (Fig. 13c).

A well-developed North Pacific High during boreal spring 1999 produced higher than normal SLP and strong anticyclonic winds over the NEP, and anomalously strong southward (upwelling-favorable) coastal winds (Figs. 5b,13d). SLPA and SSTA patterns were similar to those in the LN composite (cf. Figs. 4a,d, 12a,d). As in the 1995–97 LN and the 1997–98 EN, the characteristic spatial relationship between atmospheric and oceanic anomaly patterns indicate that SLP and low-level wind anomalies in the CNP and NEP may have contributed to the underlying upper oceanic anomalies during the 1998–2001 LN. We will discuss one possible mechanism for this relationship in the following section.

3.4. WIND STRESS CURL ANOMALIES IN THE NEP

As seen throughout section 3.3, the recurring characteristic spatial relationship between atmospheric and oceanic anomalies in the CNP and NEP indicates that anomalous surface Ekman transports may have contributed to the development of oceanic anomalies. Anomalously positive (negative) wind stress curl should produce anomalous horizontal divergence (convergence) in surface Ekman transport and a shoaling (depression) of SSH and isopycnal surfaces via Ekman pumping. To test this idea, we compared the curl of the wind stress anomalies (shown as the anomaly of the mean of the daily curl fields) and SSHAs during key phases of the EN and LN events of 1995–2001.

During much of the 1995–97 LN (e.g., November 1996–February 1997), positive curl anomalies overlaid negative SSHAs in most of the western and northeastern NEP and negative curl anomalies overlaid positive SSHAs in the NEP thermal anomaly pool (Fig. 14a). A smaller region of positive curl anomalies and negative SSHAs occurred in the southeastern NEP and coastally from Mexico to Oregon. Negative curl anomalies southwest of Alaska corresponded with another region of positive SSHA. The inverse spatial association between curl and SSH anomalies over most of the NEP suggests that anomalous Ekman processes were important during the 1995–97 LN in creating SSHAs, and more generally the thermal structure of the upper ocean in this region.

The same inverse association occurred over the NEP during the onset of the 1997–98 EN (March–May 1997) (Fig. 14b). The main curl and SSH anomaly features were similar to those during the preceding winter, but stronger and located further to the east. Negative curl anomalies now covered the CCS north of Pt. Conception, and positive SSHAs were more prevalent in this region. The onshore shift of these anomalies may have contributed, through anomalous Ekman processes, to the dramatic rise of SST and CSL anomalies in the CCS during early 1997 (Fig. 5). The strengthening and eastward shift of wind stress curl anomalies were related to larger scale changes, as indicated by the dramatic rise in the NOIx during this period (Fig. 1) and the evolution of low-level atmospheric fields over the north Pacific (cf. Figs. 6d, 8d).

During the mature phase of EN (e.g., November 1997–February 1998), wind curl and SSH anomalies still coincided spatially over most of the NEP (Fig. 14c). The major region of positive curl and negative SSH anomalies had shifted to the northeast. These anomalies were much stronger than in the preceding 12 months (cf. Fig. 14a-c), consistent with the very strong SLPAs at this time (Fig. 10d). The negative curl anomalies that previously sat southeast of the positive curl center became compressed to the south and east, and covered much of the CCS. The corresponding positive SSHAs during late 1997–early 1998 extended along the entire west coast, under this

negative curl anomaly. This correspondence indicates that anomalous Ekman processes in both the open ocean and the coastal NEP contributed to the unusually high coastal SSHs and CSLs at this time (Figs. 5c, 9c, 10c, 14c). In the mature phase of the 1997–98 EN, this buildup of SSHAs along the west coast would have added to any existing positive SSHAs due to coastal-wave activity, or even possibly misinterpreted as the remotely generated signal of a downwelling Kelvin wave.

Several previous studies have indicated that regional atmospheric forcing in the NEP is a major factor in producing oceanic anomalies during EN and LN events (e.g., Mysak, 1986; Simpson, 1992; Cayan, 1992; Miller et al., 1994). The characteristic spatial relationship between wind curl and SSH anomalies in the NEP (Fig. 14) and between anomalies in SLP, low-level winds, and upper ocean temperature (Figs. 6, 8-13) indicate that anomalous Ekman transports may have been important factors in developing oceanic anomalies. Specifically, temperature advection due to vertical and horizontal Ekman transport appears to have contributed to upper ocean temperature anomalies in the CNP and NEP. A geostrophic circulation will develop to balance the evolving Ekman mass transport, further redistributing temperature anomalies. Other regional atmosphere-ocean interaction mechanisms (e.g., sensible and latent heat flux, mixing) may have contributed to these oceanic anomalies as well (e.g., Cayan, 1992; Miller *et al.,* 1994). The relative importance of these mechanisms are being investigated in ongoing studies.

3.5. ATMOSPHERIC TELECONNECTIONS DURING 1995–2001

As discussed in section 3.3, upper tropospheric anomalies are good indicators of atmospheric teleconnections that force the NEP remotely. In this section, 200-hPa geopotential height anomalies are analyzed to define the role of these teleconnections in the production of the surface atmospheric and upper oceanic anomalies described in the previous sections.

As in the LN composite, upper tropospheric height anomalies over the north Pacific, North America, and the north Atlantic in January–March 1996 were part of a series of anomalous wave trains emanating from east Asia and the central tropical Pacific (cf. Figs. 4c and 15a). This indicates the strong height anomaly over the CNP–NEP in early 1996 had a remote origin similar to that in other LN events. However positive height anomalies over the CNP–NEP were shifted to the north and east during winter 1995–96, relative to the composite LN, roughly straddling the west coast of North America. The strongest positive height anomalies were centered near southern Alaska and southern California, with weaker negative anomalies north and southeast of Hawaii. The corresponding SLP and lower tropospheric wind anomalies (not shown) were qualitatively similar, with anticyclonic (downwelling-favorable) wind anomalies over the NEP and along most of the west coast. These west coast anomalies were consistent with the development of positive SSTAs in the

NEP, especially in the NEP thermal anomaly pool, during the first boreal winter of the 1995–97 LN.

Upper tropospheric height anomalies in the extratropical north Pacific during December 1996–January 1997 (Fig. 15b) were unlike those in the LN composite, perhaps because LN was especially weak at this time. However, as in the first winter of this LN event, positive (negative) height anomalies were centered near southern California (north of Hawaii) (cf. Figs. 15a,b). These height anomalies had counterparts in the lower atmosphere. In particular, the negative height anomaly from north of Hawaii to western Canada (Fig. 15b) was matched by negative SLP and cyclonic wind anomalies (Fig. 6d). These appear to have contributed to upper ocean temperature and SSH anomalies in the CNP–NEP (cf. Figs. 6a-c, 14a). As in winter 1995–96, the origins of the CNP–NEP anomalies may be traced back to an anomalous wave train that emanated from east Asia. No anomalous wave train originated from the central tropical Pacific, due to the weak LN state.

During July–September 1997, the 200-hPa height anomalies revealed a series of zonal anomalous wave trains emanating from east Asia and extending into the NEP (Fig. 15c). Such zonal height anomalies are a common response to anomalous tropospheric heating in southeast Asia and the western tropical Pacific, and tend to be especially clear during June–December (Nitta,1987; Ford, 2000). The anomalous wave train pattern over the NEP, North America, and the north Atlantic during August–September 1997 (Fig. 15c) is similar to the typical boreal summer–early winter EN pattern (Ford, 2000). An anomalous wave train from the central tropical Pacific into the NEP was not evident during this period. This is not surprising, since such teleconnections tend to be weak outside of the boreal winter (Horel and Wallace, 1981; Hoskins and Karoly, 1981). As in the preceding two winters, upper tropospheric and low level anomalies corresponded closely, especially the negative 200-hPa height anomalies and the underlying negative SLP and cyclonic wind anomalies in the northern NEP (cf. Figs. 9d, 15c). This correspondence indicates teleconnections from east Asia contributed to atmospheric anomalies in the NEP during summer 1997, and probably to the underlying oceanic anomalies (see sections 3.3 and 3.4).

Despite strong EN conditions in the equatorial Pacific since boreal spring 1997, a clear atmospheric teleconnection from the central tropical Pacific to the NEP did not develop until late 1997. In November 1997–February 1998, the 200-hPa height anomalies were very similar to the composite EN patterns (cf. Figs. 3c, 15d). An anomalous wave train from east Asia into the NEP was especially clear. A separate anomalous wave train from the central tropical Pacific, a feature typical of the mature phase of EN during the boreal winter (Fig. 3c), interfered constructively with the east Asian wave train over North America and the north Atlantic. The strong SLP and surface

wind anomalies that developed in the NEP during winter 1997–98 (Fig. 10d) were surface expressions of EN-induced atmospheric teleconnections.

Upper tropospheric height anomalies during much of the 1998–2001 LN (not shown) also corresponded to the major SLP and surface wind anomalies in the CNP and NEP. Throughout 1995–2001, the major surface atmospheric anomalies in the extratropical north Pacific were part of anomalous tropospheric wave trains, principally from east Asia. The impacts of these wave trains were likely important in the evolution of the upper oceanic anomalies in the NEP during this period, through their influence on surface atmospheric processes.

4. DISCUSSION

Tropical and extratropical Pacific anomalies during 1995–2001 varied strongly on intraseasonal and interannual scales (Figs. 3, 4, 5, 7). During late 1996–early 1998, equatorial internal Kelvin waves were forced by intraseasonal eastward wind bursts in the western tropical Pacific (Fig. 7, also see McPhaden, 1999; Chavez, Strutton, Friederich, Feely, Feldman, Foley, *et al.*, 1999), which are associated with 30–60 day Madden–Julian Oscillations (Madden & Julian, 1971). The downwelling phases of two prominent waves, generated in late December 1996 and early March 1997, reached South America in March and May 1997, respectively. Other downwelling Kelvin waves can be seen throughout 1997, each associated with an eastward wind burst (Fig. 7a,c). These waves may have propagated along the eastern boundary as coastal Kelvin waves, and may have been responsible for much of the positive sea level anomalies in the CCS in late spring and autumn–winter 1997–98 (Ryan & Noble, 2001; Strub & James, 2001).

Collectively these intraseasonal equatorial waves contributed to the interannual buildup of CSL and deepening thermocline at the equatorial eastern boundary during the latter half of 1997 (Fig. 7c, 8-10), which may have generated a quasi-geostrophic poleward flow into the NEP (cf., McAlpin, 1995; Clarke & Lebedev, 1999). Other equatorial thermocline anomalies tracked the eastward movement of anomalous interannual zonal winds during late 1996–early 1998 (Fig. 7a,c), taking about 18 months to cross the Pacific. A similar slow-moving signal has been seen in previous EN events (cf. Fig. 4 in Enfield, 1987). White & Cayan (2000) found interannual global tropical SST and SLP signals that propagate eastward out of phase at a similar speed. They suggest this interannual mechanism is tied to global decadal variability and has modulated past EN/LN events, and emphasize that it is very different from the mechanism traditionally credited for EN/LN variability.

Interannual variability in the NEP during the 1997–98 EN was distinguished by large regional- and basin-scale anomalies in low-level wind, upper ocean temperature, and sea level that

developed during the 1995–97 LN and persisted through early 1998 (Figs. 5, 8-10). Interannual anomalies in the coastal NEP probably were due to the combined effects of regional atmospheric and remote oceanic forcing. Regional atmospheric forcing included: (1) persistent negative SLP and cyclonic wind anomalies in the CNP-NEP from late 1996–early 1998, with especially intense anomalies in winter 1997–98 (Fig. 10); and (2) atmospheric anomalies over the open ocean that shifted onshore from winter 1996–97 through winter 1997–98 (Figs., 5-6, 8-10). Remote oceanic forcing included: (1) generation of coastal Kelvin waves by persistent eastward winds in the tropical Pacific and poleward winds in the NEP (Figs. 5-10; also McPhaden, 1999; Ryan and Noble, 2001; Strub and James, 2001); and (2) accumulation of mass and energy along the west coast as coastal Kelvin waves generated westward propagating Rossby waves (Pares-Sierra & O'Brien, 1989; Clarke & Van Gorder, 1994; McAlpin, 1995).

A major focus of this study is the degree to which atmospheric and oceanic anomalies in the NEP during 1997–98 were related to the 1997–98 EN event. Our analyses indicate that these anomalies did not have a *clear and direct* connection to tropical Pacific anomalies until boreal autumn 1997. NEP oceanic anomalies in the early phase of EN were primarily the result of: (1) pre-existing oceanic anomalies generated during the 1995–97 LN by regional atmospheric anomalies (Figs. 5-6, 14a, 15a,b); and (2) the modification of oceanic anomalies during this phase of EN by regional atmospheric anomalies that were not tied directly to the EN event (Figs. 5, 8-9, 14b, 15c).

During July–September 1997, the major atmospheric anomalies in the NEP were linked to anomalous extratropical atmospheric wave trains from East Asia (Fig. 15c). These wave trains are due to EN-related anomalies in atmospheric convection in the western tropical Pacific, and are typical during EN (Ford, 2000). Thus atmospheric anomalies in the NEP during July–September may have been linked *indirectly* to the 1997–98 EN via atmospheric teleconnections from the tropics. North Pacific anomalies during previous EN events have not always been related in obvious ways to tropical extremes, and actually may have been precursors to EN (Namias, 1976; Emery & Hamilton, 1985; White & Tabata, 1987; Simpson, 1992). During November 1997–April 1998, atmospheric wave trains from both East Asia and the central tropical Pacific were important in generating atmospheric anomalies in the NEP (Figs. 5, 10, 15d). These atmospheric anomalies were a major factor in the development of the NEP oceanic anomalies during the second half of the 1997–98 EN.

A second focus of this study is to define the relative contribution of regional atmospheric forcing and remotely forced oceanic propagations to the evolution of NEP anomalies during the 1997–98 EN. To clarify the possible sources and mechanisms of forcing in the CCS, we applied a

stepwise linear model using the central California coastal time series for 1995-1999 (Fig. 5). Anomalous CSL is the dependent variable, and buoy alongshore wind "stress" (the daily wind anomaly squared, sign preserved) and SST anomalies are the independent variables. We entered stress into the model first, then SST after pre-whitening it by removing the partial correlation with stress ($r^2 = .14$).

$$CSL(t) = \alpha + \beta_1 \cdot \text{stress}(t) + \beta_2 \cdot SST(t) \qquad \text{(Eqn. 1)}$$

The thin solid line in Figure 5c is the modeled CSL anomaly using wind alone ($r^2 = .44$); the dashed line incorporates wind and SST ($r^2 = .79$). From the time series, it is clear that local wind forcing is an important contributor to intraseasonal perturbations in CSL (e.g., strong poleward wind anomalies in May, July, and November 1997, and February 1998). However wind anomalies do not track the interannual rise and fall of CSL anomalies from early August 1997 to mid-April 1998. Local winds also underestimate the large CSL rise during the May 1997 downwelling event. The model response to SST may represent thermal and dynamical effects associated with larger scale (regional) variations in the wind (e.g., curl) and related Ekman and geostrophic transports, coastal-trapped waves, and in-situ warming, primarily on interannual scales.

Throughout the study period, atmospheric and oceanic anomalies in the CNP–NEP featured a recurring characteristic spatial relationship, and regional atmospheric forcing appears to have been a major factor in creating the underlying oceanic anomalies. The main evidence for this comes from all phases of the 1995–97 LN, 1997–98 EN, and 1998–2001 LN events.

(1) Atmospheric and upper oceanic anomalies in the CNP–NEP had a characteristic spatial relationship. When this region was dominated by negative (positive) SLP and cyclonic (anticyclonic) low-level wind anomalies, SSTAs were positive (negative) east and north, and negative (positive) west and south of the SLPA center (Figs. 6, 8, 10, 12). This relationship is typical during EN and LN events (Figs. 3, 4), and has been identified previously as a persistent pattern in the north Pacific (Namias *et al.*, 1988).

(2) Changes in upper oceanic anomalies corresponded to changes in atmospheric anomalies, as evident in their location, shape, extent, and strength (Figs. 6, 8-10). The evolution of oceanic anomalies was too fast to be explained by lateral oceanic advection of temperature anomalies.

(3) Wind stress curl and SSH anomalies indicate that regional atmospheric forcing anomalies were responsible for much of the upper oceanic anomalies in the NEP (Fig. 14).

(4) Major atmospheric anomalies over the NEP were part of atmospheric teleconnections from remote regions (Fig. 15), indicating atmospheric anomalies were not primarily the result of underlying oceanic anomalies.

There has been considerable debate about the source of anomalous west coast CSL signals during EN, and specifically on the ability of coastal Kelvin waves to propagate from the equator to the CCS. Analyses of CSL variations from prior EN events identified poleward propagations along the North American west coast (Enfield & Allen, 1980; Chelton & Davis, 1982; Meyers *et al.*, 1998), although the range of observed phase speeds (35-300 km/day) is quite large. Theoretical speeds fall at the lower end of this range (Clarke & Van Gorder, 1994; McAlpin, 1995).

Coastal propagations, possibly originating in the equatorial Pacific (e.g., Fig. 7c), appear to have been a factor in generating oceanic anomalies in the coastal NEP during the 1997–98 EN event (Ryan and Noble, 2001; Strub and James, 2001). Positive anomalies of upper ocean currents, CSL, temperature, and salinity observed in the CCS (Collins *et al.*, 2001; Huyer *et al.*, 2001; Lynn *et al.*, 1998; Lynn & Bograd, 2001; Ryan and Noble, 2001; Strub and James, 2001) support the idea of a large-scale anomalous poleward flow from about May 1997 through February 1998. This flow would be consistent with the downwelling phase of an internal Kelvin wave. Yet the sources of and mechanisms responsible for these anomalies are not clear. Two mechanisms may explain how tropical EN signals could influence the NEP via an oceanic teleconnection along the eastern boundary. Both favor interannual over higher frequency variations in the CCS.

(1) A number of studies have determined that coastal wave energy cannot propagate effectively from the tropics to the mid-latitudes (Baumgartner & Christensen, 1985; Mysak, 1986; Spillane, Enfield, & Allen, 1987; McAlpin, 1995; Clarke & Lebedev, 1999). Cane & Sarachik (1977) defined a “critical latitude” that is a function of frequency and coastal orientation. Poleward of this latitude, Kelvin waves are coastal-trapped as a poleward subsurface jet (Clarke & Van Gorder, 1994; McAlpin, 1995), and local wind forcing will dominate CSL variability. This latitude is roughly central California (ca. 35–40°) for interannual periods, but confined to within about 20° of the equator on intraseasonal scales. Thus interannual Kelvin waves are more likely to be detected in west coast CSL anomalies.

(2) At very low frequencies, coastal waves are quasi-steady and the flow along an eastern boundary must be nearly geostrophic (McAlpin, 1995; Clarke & Lebedev, 1999). During EN, this quasi-geostrophic flow will transport warmer, more saline water poleward on interannual scales (cf. Collins *et al.*, 2001; Huyer *et al.*, 2001; Lynn & Bograd, 2001). CSL will increase (e.g., Fig. 5) in geostrophic balance with this large-scale, low-frequency anomaly in California Current transport.

However surface anomalies on shorter time scales may be more controlled by local and regional wind processes.

Coastal Kelvin waves are scattered into Rossby and coastal-trapped wave modes as they propagate poleward (Pares-Sierra & O'Brien, 1989; Clarke & Van Gorder, 1994; McAlpin, 1995). Internal Rossby waves move slowly westward (about 5 km/day at mid-latitudes), and create a coastal field much wider than the Kelvin wave decay scale that is apparent months after its generation. Such a Rossby wave signal may have been part of the SSHA fields during 1997 (Strub & James, 2001), and the CCS dynamic height fields of past EN events (Simpson, 1992; Lynn *et al*., 1995). It may have been manifested as the interannual rise and fall of central California CSL and SST as well (Fig. 5c; also Ryan and Noble, 2001).

Miller *et al*. (1997) propose an alternate mechanism for generating extratropical SSHAs during EN. Their simulations indicate that large-scale thermocline adjustments in the interior of the north Pacific, forced by wind stress curl and heat flux anomalies, excite compensatory westward-propagating baroclinic waves near the coast. Forcing from the tropical ocean contributes only weakly to extratropical thermocline anomalies. This model can account for observed west coast sea level and thermocline anomalies, and the discrepancy in phase speed between observations and theoretical scattered Rossby waves. Coastal NEP anomalies were affected by onshore shifts of open oceanic anomalies during summer–autumn 1997, as atmospheric anomalies shifted onshore (Figs. 9, 10, 14c), in a manner consistent with Miller *et al*. (1997). This coincided with the arrival of coastal propagations from the tropical Pacific (cf. Ryan & Noble, 2001; Strub & James, 2001).

Since late 1998, Pacific atmospheric and oceanic anomaly fields have displayed a typical LN pattern (cf. Figs. 2, 12-13). As of April 2001, the MEI had remained negative for 33 consecutive months, the longest continuous negative phase since 1973–76 (Figs. 1, 2). It weakened considerably in early 1999 and 2000, only to be followed by revived LN conditions. These persistent anomalies may be the early sign of a decadal climate shift. The most familiar decadal shift in the north Pacific occurred about 1977 (cf. Trenberth & Hurrell, 1994; Mantua, Hare, Zhang, Wallace, & Francis, 1997; Parrish, Schwing, & Mendelssohn, 2000). Another significant shift occurred around 1990 (Hare & Mantua, 2000; McFarlane, King, & Beamish, 2000). Minobe (1999) has identified an interdecadal oscillation in the Aleutian Low as a likely indicator of climate shifts, and suggested a phase reversal could occur as early as 1999–2000. A number of coincident biological changes along the west coast indicate major shifts in long-term ecosystem patterns since 1998 (Schwing & Moore, 2000; Schwing *et al*., 2000). Most of these are consistent with those identified with historical cooler conditions in the NEP. The large physical and biological shifts in

recent years demonstrate that the large-scale climate, and ecological conditions in the coastal NEP, can change swiftly and dramatically.

5. SUMMARY

Throughout 1995–2001, tropical and extratropical Pacific anomalies in SLP, low-level wind, upper ocean temperature, and SSH varied strongly on intraseasonal and interannual scales. Atmospheric and oceanic anomalies in the NEP featured a recurring characteristic spatial relationship, and regional atmospheric forcing appears to have been a major factor in generating the underlying oceanic anomalies. During the 1995-97 LN and 1997-98 EN, the NEP was dominated by negative SLP and cyclonic wind anomalies. Upper ocean temperature anomalies were positive along the west coast of North America, and negative in the central north Pacific. A negative regional wind stress curl anomaly, conducive to reduced Ekman pumping in the proximity of the NEP thermal anomaly pool, was an important factor in establishing and strengthening the upper oceanic anomalies that persisted well into the 1997–98 EN.

North Pacific anomalies during the 1995–97 LN resembled the typical LN pattern, shifted to the east. This eastward relocation was related to a similar shift in the atmospheric teleconnection out of east Asia. During the early phase of the 1997–98 EN, the highest temperature and SSH anomalies were offshore in the NEP thermal anomaly pool. An unusually weak North Pacific High associated with anomalous wave trains out of east Asia resulted in anomalous cyclonic atmospheric circulation. This led to weak upwelling-favorable wind stress along the coast and an intensification of negative Ekman pumping anomalies offshore. Summer 1997 was marked by a gradual eastward shift in the atmospheric anomaly pattern, and a corresponding onshore evolution of the strongest oceanic anomalies.

The processes responsible for NEP oceanic anomalies differed in the early and latter stages of the 1997–98 EN. NEP anomalies did not display a clear and direct connection to equatorial Pacific anomalies until late 1997. Prior to November 1997, upper oceanic conditions were controlled by local atmospheric forcing anomalies that were teleconnectioned to east Asia; a teleconnection from the central tropical Pacific was not evident. Beginning in November, anomalous atmospheric wave trains from east Asia and the central tropical Pacific combined to generate anomalies in the NEP. An interannual increase in sea level during the mature phase of EN appeared to be the joint effect of regional atmospheric forcing and remote coastal oceanic propagations. The two distinct types of exotic species visiting the CCS in 1997 and 1998 (Pearcy, 2001) were consistent with this change in forcing.

The concurrent development of intraseasonal equatorial sea level and extratropical wind anomalies during the 1997–98 EN makes it difficult to separate their influence on the CCS. One complicating factor is the teleconnection between tropical and extratropical atmospheric anomalies. Equatorial wind anomalies initiate separate atmospheric and oceanic teleconnections; both ultimately impact extratropical coastal ocean conditions. It may be impossible to determine the relative contribution from each path, especially since many of the intermediate signals are correlated. Nevertheless, it is reasonable to say that the observed anomalies in the CCS during the 1997–98 EN were the result of a complex blend of local atmospheric forcing, some of which was teleconnected from the tropical Pacific and east Asia, and remotely forced oceanic signals along the eastern boundary.

ACKNOWLEDGEMENTS

This research was funded as part of the US GLOBEC Northeast Pacific Project, with support from the NSF Division of Ocean Sciences and the NOAA Coastal Ocean Program Office, and by the NOAA–NMFS Pacific Fisheries Environmental Laboratory of the Southwest Fisheries Science Center (SWFSC). The authors thank Steven Cummings (NOAA/NMFS PFEL) for his assistance with the preparation of figures and the manuscript. Thanks to Cathy Smith (NOAA–CIRES Climate Diagnostics Center) for developing the global fields and methods used to compute the global correlation maps. A number of figures are based on images provided by the NOAA–CIRES CDC (http://www.cdc.noaa.gov/). Connie Fey (Scripps Institution of Oceanography) and Steven Bograd (PFEL) assisted in data acquisition. Dai McClurg and Michael McPhaden (NOAA/PMEL) provided data for the preparation of Figure 7. Ron Lynn (SWFSC); Ted Strub and Adriana Huyer (Oregon State University); Curtis Collins and Bruce Ford (NPS); Steven Bograd, Roy Mendelssohn, Richard Parrish, and Chris Moore (PFEL); and Norm Hoffmann (National Weather Service) provided many useful comments and critiques. Three anonymous referees carefully reviewed the manuscript and made a number of suggestions that greatly improved the final version. This is contribution number XXXX of the U.S. GLOBEC program, jointly funded by the National Science Foundation and National Oceanic and Atmospheric Administration.

REFERENCES

Barnston, A.G., Glantz, M.H., & He, Y. (1999). Predictive skill of statistical and dynamical climate models in SST forecasts during the 1997–98 El Niño episode and the 1998 La Niña onset. *Bulletin of the American Meteorological Society,* 80, 1829-1852.

Baumgartner, T.R., & Christensen, Jr, N. (1985). Coupling of the Gulf of California to large-scale interannual climatic variability. *Journal of Marine Research,* 43, 825-848.

Bjerknes, J. (1969). Atmospheric teleconnections from the equatorial Pacific. *Monthly Weather Review,* 97, 163-172.

Cane, M.A., & Sarachik, E.S. (1977). Forced baroclinic ocean motions. II: the linear bounded case. *Journal of Marine Research,* 35, 395-432.

Cayan, D. R. (1992). Latent and sensible heat flux anomalies over the northern oceans, *Journal of Climate, 5*, 354-369.

Chavez, F. (1996). Forcing and biological impact of onset of the 1992 El Niño in central California. *Geophysical Research Letters,* 23, 265-268.

Chavez, F.P., Strutton, P.G., & McPhaden, M.J. (1998). Biological-physical coupling in the central equatorial Pacific during the onset of the 1997–98 El Niño. *Geophysical Research Letters,* 25, 3543-3546.

Chavez, F.P., Strutton, P.G., Friederich, G.E., Feely, R.A., Feldman, G.C., Foley, D.G., & McPhaden, M.J. (1999). Biological and chemical response of the equatorial Pacific Ocean to the 1997–98 El Niño. *Science,* 286, 2126-2131.

Chelton, D.B., & Davis, R.E. (1982). Monthly mean sea-level variability along the west coast of North America. *Journal of Physical Oceanography,* 12, 757-784.

Chelton, D.B., Bernal, P.A., & McGowan, J.A. (1982). Large-scale interannual physical and biological interaction in the California Current. *Journal of Marine Research,* 40, 1095-1125.

Clarke, A.J., & Van Gorder, S. (1994). On ENSO coastal currents and sea levels. *Journal of Physical Oceanography,* 24, 661-680.

Clarke, A.J., & Lebedev, A. (1999). Remotely driven decadal and longer changes in coastal Pacific waters of the Americas. *Journal of Physical Oceanography,* 29, 828-835.

Collins, C.A., Castro, C.G., Asanuma, H., Rago, T.A., Han, S.-K., Durazo, R., & Chavez, F.P. (2001). Changes in the Hydrography of Central California Waters Associated with the 1997-8 El Niño. submitted to *Progress in Oceanography*.

Dorman, C.E., & Winant, C.D. (1995). Buoy observations of the atmosphere along the west coast of the United States, 1981–1990. *Journal of Geophysical Research,* 100, 16029-16044.

Emery, W., & Hamilton, D. (1985). Atmospheric forcing of interannual variability in the northeast Pacific Ocean: Connections with El Niño. *Journal of Geophysical Research,* 90, 857-868.

Enfield, D.B. (1987). The intraseasonal oscillation in eastern Pacific sea levels: how is it forced? *Journal of Physical Oceanography,* 17, 1860-1876.

Enfield, D.B., & Allen, J.S. (1980). On the structure and dynamics of monthly mean sea level anomalies along the Pacific coast of North and South America. *Journal of Physical Oceanography,* 10, 557-578.

Ford, B. (2000). El Niño and La Niña Effects on Tropical Cyclones: The Mechanisms. M.S. Thesis, Naval Postgraduate School, Monterey CA, unpublished.

Hare, S.R., & Mantua, N.J. (2000). Empirical evidence for North Pacific regime shifts in 1977 and 1989, *Progress in Oceanography,* 47, 103-145.

Hartmann, D., (1994). *Global Physical Climatology*. New York: Academic Press

Hoskins, B.J., & Karoly., D.J. (1981). The steady linear response of a spherical atmosphere to thermal and orographic forcing. *Journal of Atmospheric Science,* 38, 1179-1196.

Hayward, T.L., Baumgartner, T.R., Checkley, D.M., Durazo, R., Gaxiola-Castro, G. , Hyrenbach, K.D., Mantyla, A.W., Mullin, M.M., Murphree, T., Schwing, F.B., Smith, P.E., & Tegner, M. (1999). The state of the California Current, 1998–1999: transition to cool water conditions. *California Cooperative Oceanic Fisheries Investigations Reports,* 40, 29-62.

Horel, J., & Wallace, J. M. (1981). Planetary-scale atmospheric phenomena associated with the Southern Oscillation. *Monthly Weather Review,* 109, 813-829.

Huyer, A., Smith, R.L., & Fleischbein, J. (2001). The coastal ocean off Oregon and northern California during the 1997–8 El Niño. submitted to *Progress in Oceanography*.

Kalnay, E., & Coauthors. (1996). The NCEP/NCAR Reanalysis 40-year Project. *Bulletin of the American Meteorological Society,* 77, 437-471.

Kudela, R.M., & Chavez, F.P. (2000). Modeling the impact of the 1992 El Niño on new production in Monterey Bay, California. *Deep-Sea Research II,* 47, 1055-1076.

Levitus, S., Boyer, T.P., Conkright, M.E., O' Brien, T., Antonov, J., Stephens, C., Stathopolos, L., Johnson, D., & Gelfeld, R. (1998). *NOAA Atlas NESDIS 18,World Ocean Database 1998: Volume 1: Introduction*., Washington, DC: U.S. Gov. Printing Office.

Lynn, R.J., Schwing, F.B., & Hayward, T.L. (1995). The effect of the 1991–93 ENSO on the California Current System. *California Cooperative Oceanic Fisheries Investigations Reports,* 36, 57-71.

Lynn, R.J., Baumgartner, T., Collins, C.A., Garcia. J., Hayward, T.L., Hyrenbach, K.D. , Mantyla, A.W., Murphree, T., Shankle, A., Schwing, F.B., Sakuma, K.M., & Tegner, M. (1998). The state of the

California Current, 1997–1998: transition to El Niño conditions. *California Cooperative Oceanic Fisheries Investigations Reports,* 39, 25-49.

Lynn, R.J., & Bograd, S.J. (2001). Dynamic evolution of the 1997–99 El Niño–La Niña cycle in the southern California Current System. submitted to *Progress in Oceanography*.

Mantua, N., Hare, S., Zhang, Y., Wallace, J., & Francis, R. (1997). A Pacific interdecadal climate oscillation with impacts on salmon production. *Bulletin of the American Meteorological Society,* 78, 1069-1079.

Madden, R.A., & Julian, P.R. (1971). Detection of a 40–50 day oscillation in the zonal wind in the tropical Pacific. *Journal of Atmospheric Science,* 28, 702-708.

McAlpin, J.D. (1995). Rossby wave generation by poleward propagating Kelvin waves: the midlatitude quasigeostrophic approximation. *Journal of Physical Oceanography,* 25, 1415-1425.

McFarlane, G.A., King, J.R., & Beamish, R.J. (2000). Have there been recent changes in climate? Ask the fish. *Progress in Oceanography,* 47, 147-169.

McPhaden, M.J. (1999). Genesis and evolution of the 1997–98 El Niño. *Science,* 283, 950-954.

Meyers, S.D., Melsom, A., Mitchum, G.T., & O'Brien, J.J. (1998). Detection of the fast Kelvin wave teleconnection due to El Niño–Southern Oscillation. *Journal of Geophysical Research,* 103, 27655-27663.

Miller, A. J., Cayan, D. C., Barnett, T. P., Graham, N. E., & Oberhuber, J. M. (1994). Interdecadal variability of the Pacific Ocean: model response to observed heat flux and wind stress anomalies, *Climate Dynamics,* 9, 287-302.

Miller, A.J., White, W.B., & Cayan, D.R. (1997). North Pacific thermocline variations on ENSO time scales. *Journal of Physical Oceanography,* 27, 2023-2039.

Miller, A.J. & Schneider, N. (2000). Interdecadal climate regime dynamics in the North Pacific Ocean: theories, observations and ecosystem impacts, *Progress in Oceanography,* 47, 355-379.

Minobe, S. (1999). Resonance in bidecadal and pentadecadal climate oscillations over the north Pacific: role in climate regime shifts. *Geophysical Research Letters,* 26, 855-858.

Murphree, T., & Reynolds, C. (1995). El Niño and La Niña effects on the northeast Pacific: The 1991–1993 and 1988–1989 events. *California Cooperative Oceanic Fisheries Investigations Reports,* 36, 45-56.

Murphree, T., & Schwing, F. (2001). The role of extratropical Pacific anomalies in the initiation of El Niño and La Niña events. submitted to *Journal of Climate*.

Murphree, T., Schwing, F., & deWitt, L. (2001). Multiple wave trains and the analysis of teleconnections during El Niño and La Niña. submitted to *Journal of Climate*.

Mysak, L. (1986). El Niño, interannual variability and fisheries in the northeast Pacific Ocean. *Canadian Journal of Fisheries and Aquatic Science,* 43, 464-497.

Namias, J. (1976). Some statistical and synoptic characteristics associated with El Niño. *Journal of Physical Oceanography,* 6, 130-138.

Namias, J., Yuan, X., & Cayan, D.R. (1988). Persistence of north Pacific sea surface temperature and atmospheric flow patterns. *Journal of Climate,* 1, 682-703.

Nitta, T. (1987). Convective activities in the tropical western Pacific and their impact on the northern hemisphere summer circulation. *Journal of the Meteorological Society of Japan,* 65, 373-390.

Pares-Sierra, A., & O'Brien, J. (1989). The seasonal and interannual variability of the California Current System: a numerical model. *Journal of Geophysical Research,* 94, 3159-3180.

Parrish, R.H., Schwing, F.B., & Mendelssohn, R. (2000. Midlatitude wind stress: the energy source for climatic regimes in the North Pacific Ocean. *Fisheries Oceanography,* 9, 224-238.

Pearcy, W.G. (2001). Effects of the 1997–98 El Niño on marine nekton off Oregon. submitted to *Progress in Oceanography*.

Pearcy, W.G., & Schoener, A. (1987). Changes in the marine biota coincident with the 1982–1983 El Niño in the northeastern Pacific Ocean. *Journal of Geophysical Research,* 92, 14417-14428.

Peixoto, J., & Oort, A. (1992). *Physics of Climate*. Woodbury, NY: American Institute of Physics.

Philander. G. (1990). *El Niño, La Niña, and the Southern Oscillation*. San Diego, CA: Academic.

Plumb, A.J. (1985). On the three dimensional propagation of stationary waves. *Journal of Atmospheric Science,* 42, 217-229.

Rassmusson, E. M., & Carpenter, T. H. (1982). Variations in tropical seas surface temperature and surface wind fields associated with the Southern Oscillation/El Niño. *Monthly Weather Review,* 110, 354-384.

Ryan, H.F., & Noble, M. (2001). Sea level response to ENSO along the central California coast: how the 1997-98 event compares to the historic record. submitted to *Progress in Oceanography*.

Schwing, F., & Ralston, S. (1995). The 1991–92 El Niño and its impact on fisheries. *California Cooperative Oceanic Fisheries Investigations Reports,* 36, 43.

Schwing, F.B. and C.S. Moore. (2000). A year without summer for California, or a harbinger of a climate shift? *Transactions, American Geophysical Union,* 81(27), 301ff.

Schwing, F., Moore, C., Ralston, S., & Sakuma, K.A. (2000). Record Coastal Upwelling in the California Current in 1999. *California Cooperative Oceanic Fisheries Investigations Reports,* 41, 148-160.

Schwing, F.B., Murphree, T., & Green, P.M. (2001). The Northern Oscillation Index: a climate index for the northeast Pacific. *Progress in Oceanography*, in press.

Sette, O.E., & Isaacs, J.D., eds. (1960). Symposium of the changing Pacific Ocean in 1957 and 1958. *California Cooperative Oceanic Fisheries Investigations Reports,* 7, 13ff.

Simpson, J.J. (1992). Response of the southern California Current system to the mid-latitude North Pacific coastal warming events of 1982–1983 and 1940–1941. *Fisheries Oceanography,* 1, 57-79.

Spillane, M.C., Enfield, D.B., & Allen, J.S. (1987). Intraseasonal oscillations in sea level along the west coast of the Americas. *Journal of Physical Oceanography,* 17, 313-325.

Strub, P.T., & James, C. (2001). Altimeter-derived surface circulation in the large-scale NE Pacific gyres: Part 2. 1997–1998 El Niño anomalies. submitted to *Progress in Oceanography*.

Trenberth, K.E. (1997). The definition of El Niño. *Bulletin of the American Meteorological Society*, 78, 2771-2777.

Trenberth, K.E., & Hurrell, J.W. (1994). Decadal atmospheric-ocean variations in the Pacific. *Climate Dynamics,* 9, 303-319.

Wallace, J. M., & Gutzler, D. S. (1981). Teleconnections in the geopotential height field during the Northern Hemisphere winter. *Monthly Weather Review,* 109, 784-812.

White, W.B., & Tabata, S. (1987). Interannual westward-propagating baroclinic long-wave activity on Line P in the eastern midlatitude north Pacific. *Journal of Physical Oceanography,* 17, 385-396.

White, W.B., & Cayan, D.R. (2000). A global El Niño–Southern Oscillation wave in surface temperature and its interdecadal modulation from 1900 to 1997. *Journal of Geophysical Research,* 105, 11223-11242.

Wolter, K., & Timlin, M.S. (1998). Measuring the strength of ENSO– how does 1997/98 rank? *Weather,* 53, 315-324.

Wooster, W.S., & Fluharty, D.L., eds. (1985). *El Niño North: Niño Effects in the Eastern Subarctic Pacific Ocean*. Seattle, WA: Washington Sea Grant Program.

FIGURE CAPTIONS

Figure 1. Monthly Multivariate ENSO Index (MEI, broken line) and extratropical Northern Oscillation Index (NOIx, solid line) for January 1995–January 2001. Shading denotes mature EN and LN periods.

Figure 2. MEI comparing 1997–98 EN to previous ENs (upper panel). MEI comparing 1995–97 and 1998–2000 LN to previous LNs (lower panel). Thick white vertical line in lower panel is not meant to represent separate LN events, but separates two 12-month periods within the individual LN events.

Figure 3. Composite EN anomalies during November-February, based on the EN events given in Table 3. Anomalies of: a) SST (°C); b) ocean temperature (°C) at 100 m depth; c) geopotential height (m) at 200 hPa; and d) sea level atmospheric pressure (SLP, in hPa) and wind velocity (m/s) at 850 hPa. Wind anomalies indicate lower atmospheric anomalies, with vector scale shown in upper-left box. Warm (cool) colors indicate positive (negative) temperature, height, and SLP anomalies, with scales shown to right of panels. In panel c: H (L) denotes center of a positive (negative) height anomaly in anomalous wave trains that affect the NEP; arrows show schematically the propagation of anomalous planetary wave energy through the anomalous wave trains that affected the NEP, based on analyses of quasi-geostrophic wave activity flux vectors (Plumb, 1985); and the box denotes region covered by other panels.

Figure 4. As for Figure 1, for composite of past La Niña events given in Table 3.

Figure 5. Daily time series of regional composite anomalies of: a) alongshore (positive poleward) component of NDBC coastal buoy wind; b) NDBC coastal buoy SST; and c) coastal sea level along central California, 1995–99. Locations used to create composite series shown in Table 1. Gray shading denotes mature La Niña and El Niño periods. Black bars are periods of composite maps. Bold line in panel a is 90-day running mean of daily wind anomalies (fine line). Bold solid line in panel c is CSL time series. Thin solid line is CSL estimated from wind "stress" (daily wind anomaly squared) alone. Dashed line is CSL estimated from stress and SST anomalies.

Figure 6. Pacific Ocean anomaly fields for November 1996–February 1997 of: a) SST (°C); b) ocean temperature (°C) at 100 m depth; c) sea surface height (SSH) (cm); and d) SLP (hPa) and wind velocity (m/s) at 850 hPa. Wind anomalies indicate lower atmospheric anomalies, with vector scale shown in upper left box. Warm (cool) colors indicate positive (negative) temperature, SSH, and SLP anomalies, with scales shown to right of panels.

Figure 7. Time/longitude plots of equatorial (2°N–2°S) anomalies of: a) surface zonal wind (m/s); b) SST (°C); and c) 20°C isotherm depth (m), January 1995–July 2000. Analyses based on 5-day averages of moored time series data from the TAO/TRITON array. Warm colors indicate eastward wind, warm SST, and deep thermocline anomalies. The 20°C isotherm represents the approximate depth of the main thermocline, so a positive (negative) anomaly in the depth of this isotherm corresponds to a deeper (shallower) thermocline and a warmer (cooler) upper ocean. Analyses provided by Michael J. McPhaden (NOAA/PMEL).

Figure 8. As for Figure 6, for March–May 1997.

Figure 9. As for Figure 6, for July–September 1997.

Figure 10. As for Figure 6, for November 1997–February 1998.

Figure 11. As for Figure 6, for June–August 1998.

Figure 12. As for Figure 6, for November 1998–February 1999.

Figure 13. As for Figure 6, for April–June 1999.

Figure 14. SSHAs and wind stress curl anomalies for the NEP for: a) November 1996–February 1997; b) March–May 1997; and c) November 1997–February 1998. Contours denote magnitude of curl anomaly. Contour interval is 0.2×10^{-7} Pa/m. Dashed contours denote negative curl anomaly. Warm (cool) colors indicate higher (lower) than normal SSHs, with scale shown at right.

Figure 15. Anomalous 200-hPa geopotential heights (m) for: a) January–March 1996; b) December 1996–January 1997; c) August–September 1997; and d) November 1997–February 1998. Warm (cool) colors indicate higher (lower) than normal heights, with scale shown at bottom. Arrows show schematically the propagation of anomalous planetary wave energy through the anomalous wave trains that affected the NEP, based on analyses of quasi-geostrophic wave activity flux vectors (Plumb, 1985). Vertical lines at 120°E and 70°W denote zonal extent of Pacific region shown in previous figures.

TABLE 1. NDBC buoys used in the creation of the composite wind and SST time series. Angle denotes the positive direction of alongshore wind component used for each series, based on the maximum variance.

BUOY	POSITION	ANGLE (N°)
Bodega (46013)	38.2°N 123.3°W	312
San Francisco (46026)	37.7°N 122.8°W	309
Santa Cruz (46012)	37.4°N 122.7°W	332
Monterey (46042)	36.7°N 122.4°W	328
Cape San Martin (46028)	35.7°N 121.9°W	321
Santa Maria (46011)	34.9°N 120.9°W	325

TABLE 2. Phases of La Niña and El Niño, 1995–2000, based on the Multivariate ENSO Index (MEI) (Fig. 1).

		Period
1995–1997 LN		
1	Mature, but weak to moderately strong	9/95 – 2/97
1997–1998 EN		
2	Very rapid growth, from neutral to strong	3/97 – 6/97
3 a	Mature, very strong	7/97 – 9/97
b	Mature, very strong but slightly weaker	10/97 – 12/97
c	Mature, very strong	1/98 – 3/98
4 a	Rapid decay, from strong to neutral	4/98 – 7/98
1998–2001 LN		
4 b	Rapid growth, from neutral to strong	8/98 – 10/98
5 a	Mature, strong	11/98 – 3/99
b	Mature, weak to moderately strong	4/99 – 9/99
c	Mature, moderately strong	10/99 – 3/00

TABLE 3. Periods used to create November–February composite El Niño and La Niña anomaly fields in Figures 3 and 4.

El Niño	La Niña
1965–66	1961–62
1972–73	1962–63
1976–77	1964–65
1977–78	1970–71
1979–80	1971–72
1982–83	1973–74
1986–87	1974–75
1987–88	1975–76
1991–92	1984–85
1992–93	1988–89

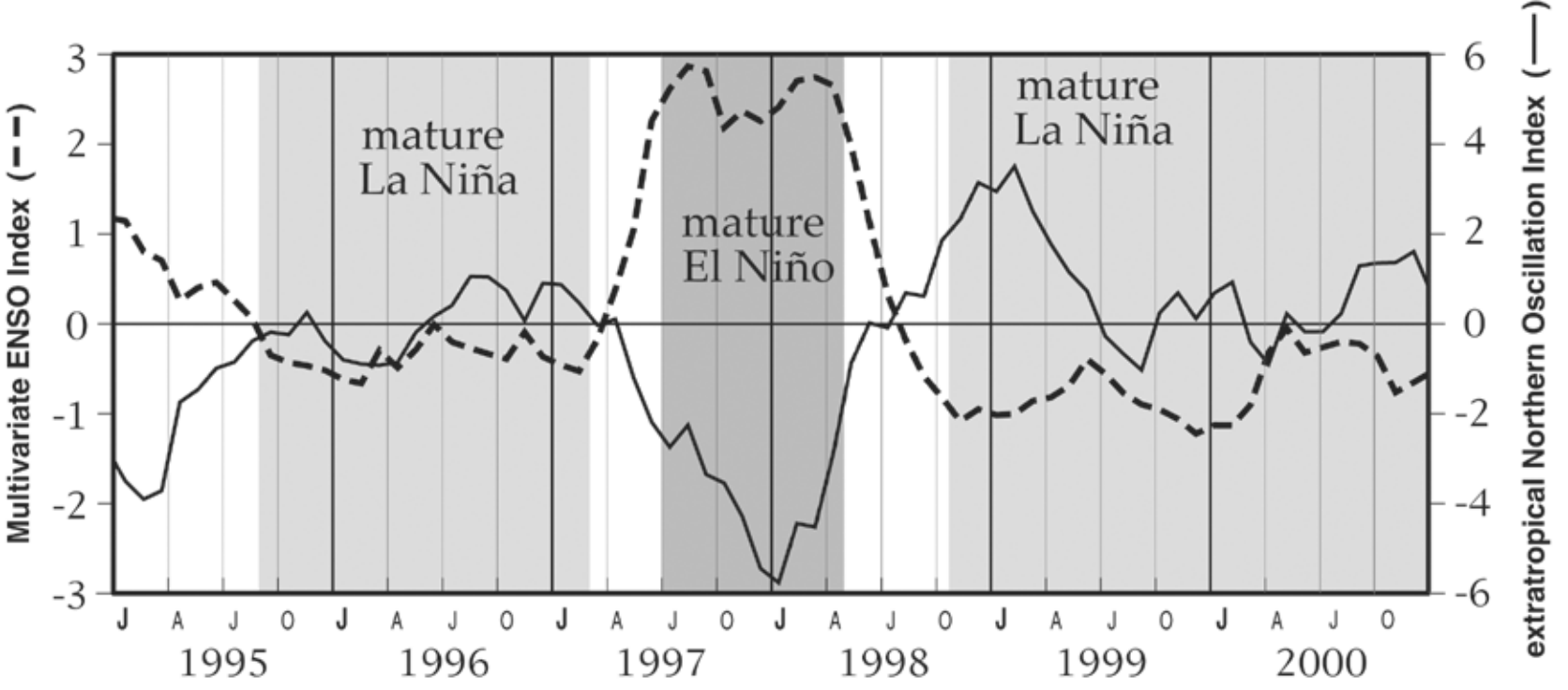
Multivariate ENSO Index (– –)
extratropical Northern Oscillation Index (——)
3
2
1
0
-1
-2
-3
6
4
2
0
-2
-4
-6
mature
La Niña
mature
El Niño
mature
La Niña
J A J O J A J O J A J O J A J O J A J O J A J O
1995
1996
1997
1998
1999
2000

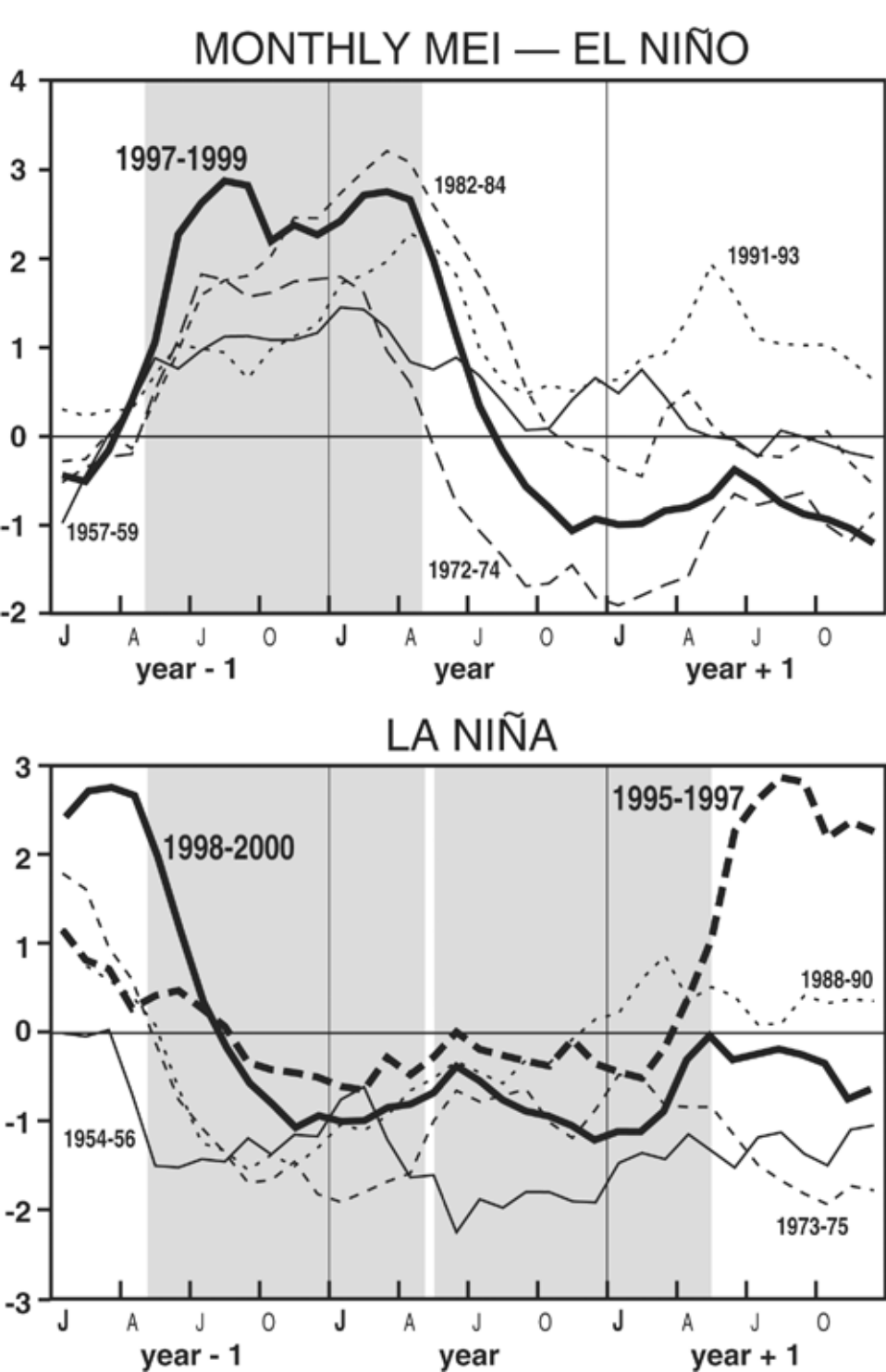
MONTHLY MEI — EL NIÑO
4
3
2
1
0
-1
-2
1997-1999
1982-84
1991-93
1957-59
1972-74
J A J O J A J O J A J O
year - 1
year
year + 1
LA NIÑA
3
2
1
0
-1
-2
-3
1998-2000
1995-1997
1988-90
1954-56
1973-75
J A J O J A J O J A J O
year - 1
year
year + 1

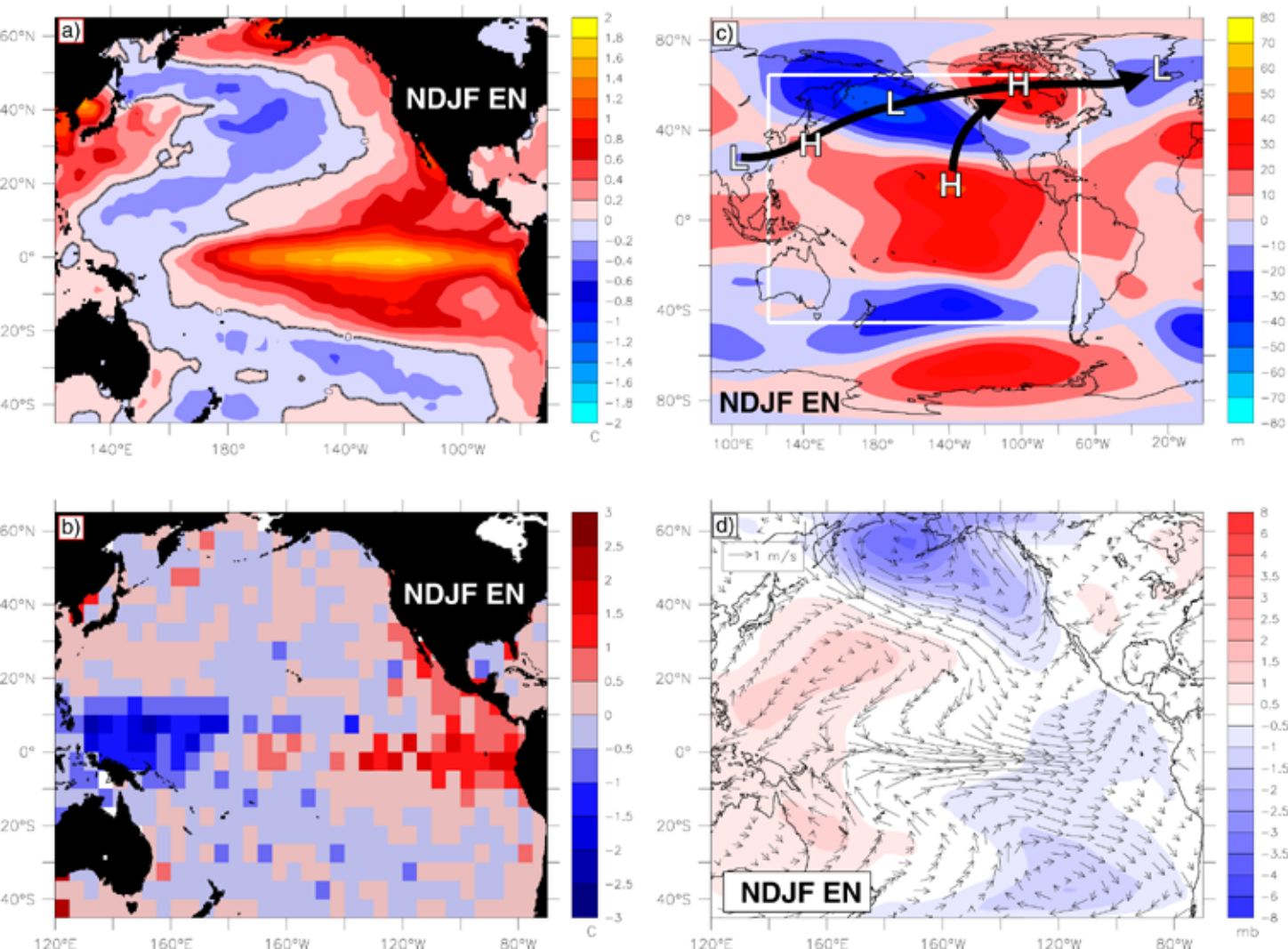
a)
NDJF EN
60°N
40°N
20°N
0°
20°S
40°S
140°E
180°
140°W
100°W
2
1.8
1.6
1.4
1.2
1
0.8
0.6
0.4
0.2
0
−0.2
−0.4
−0.6
−0.8
−1
−1.2
−1.4
−1.6
−1.8
−2
C
c)
L
H
L
H
H
L
NDJF EN
80°N
40°N
0°
40°S
80°S
100°E
140°E
180°
140°W
100°W
60°W
20°W
80
70
60
50
40
30
20
10
0
−10
−20
−30
−40
−50
−60
−70
−80
m
b)
NDJF EN
60°N
40°N
20°N
0°
20°S
40°S
120°E
160°E
160°W
120°W
80°W
3
2.5
2
1.5
1
0.5
0
−0.5
−1
−1.5
−2
−2.5
−3
C
d)
1 m/s
NDJF EN
60°N
40°N
20°N
0°
20°S
40°S
120°E
160°E
160°W
120°W
80°W
8
6
4
3.5
3
2.5
2
1.5
1
0.5
−0.5
−1
−1.5
−2
−2.5
−3
−3.5
−4
−6
−8
mb

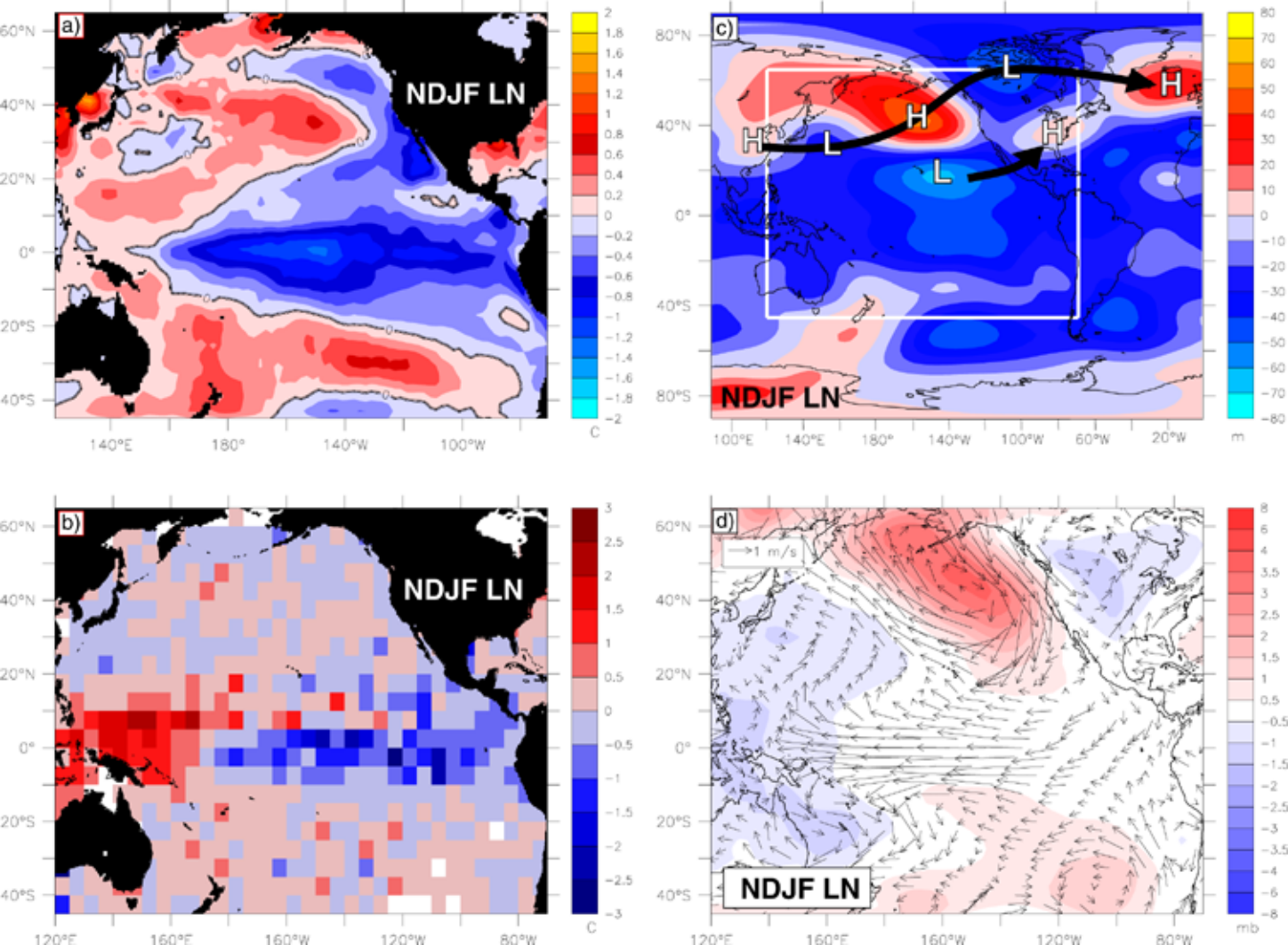
a)
NDJF LN
60°N
40°N
20°N
0°
20°S
40°S
140°E
180°
140°W
100°W
2
1.8
1.6
1.4
1.2
1
0.8
0.6
0.4
0.2
0
−0.2
−0.4
−0.6
−0.8
−1
−1.2
−1.4
−1.6
−1.8
−2
C
c)
L
H
H
L
H
L
H
NDJF LN
80°N
40°N
0°
40°S
80°S
100°E
140°E
180°
140°W
100°W
60°W
20°W
80
70
60
50
40
30
20
10
0
−10
−20
−30
−40
−50
−60
−70
−80
m
b)
NDJF LN
60°N
40°N
20°N
0°
20°S
40°S
120°E
160°E
160°W
120°W
80°W
3
2.5
2
1.5
1
0.5
0
−0.5
−1
−1.5
−2
−2.5
−3
C
d)
1 m/s
NDJF LN
60°N
40°N
20°N
0°
20°S
40°S
120°E
160°E
160°W
120°W
80°W
8
6
4
3.5
3
2.5
2
1.5
1
0.5
−0.5
−1
−1.5
−2
−2.5
−3
−3.5
−4
−6
−8
mb

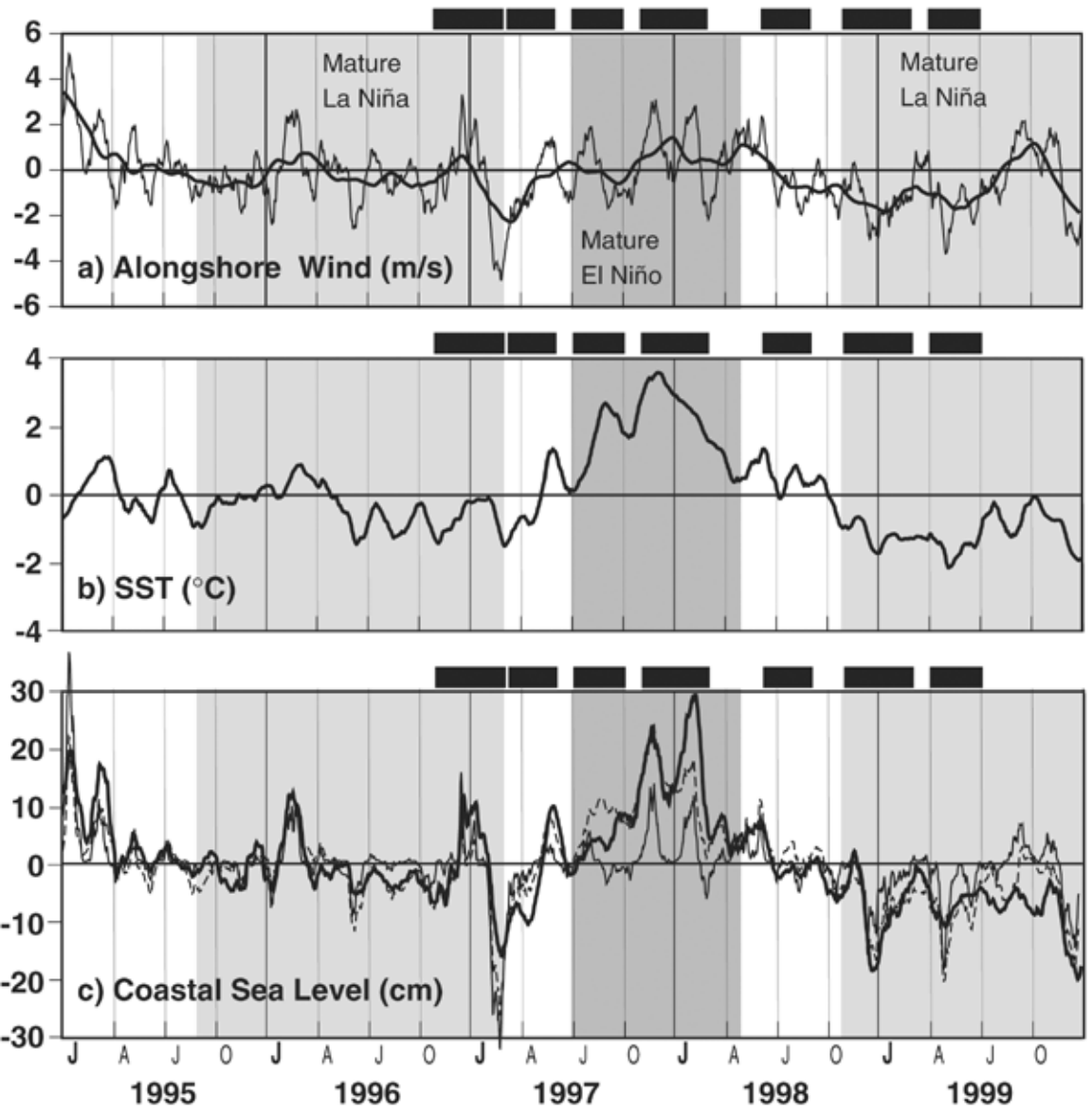
Mature
La Niña
Mature
El Niño
Mature
La Niña
a) Alongshore Wind (m/s)
b) SST (°C)
c) Coastal Sea Level (cm)
J A J O J A J O J A J O J A J O J A J O
1995
1996
1997
1998
1999

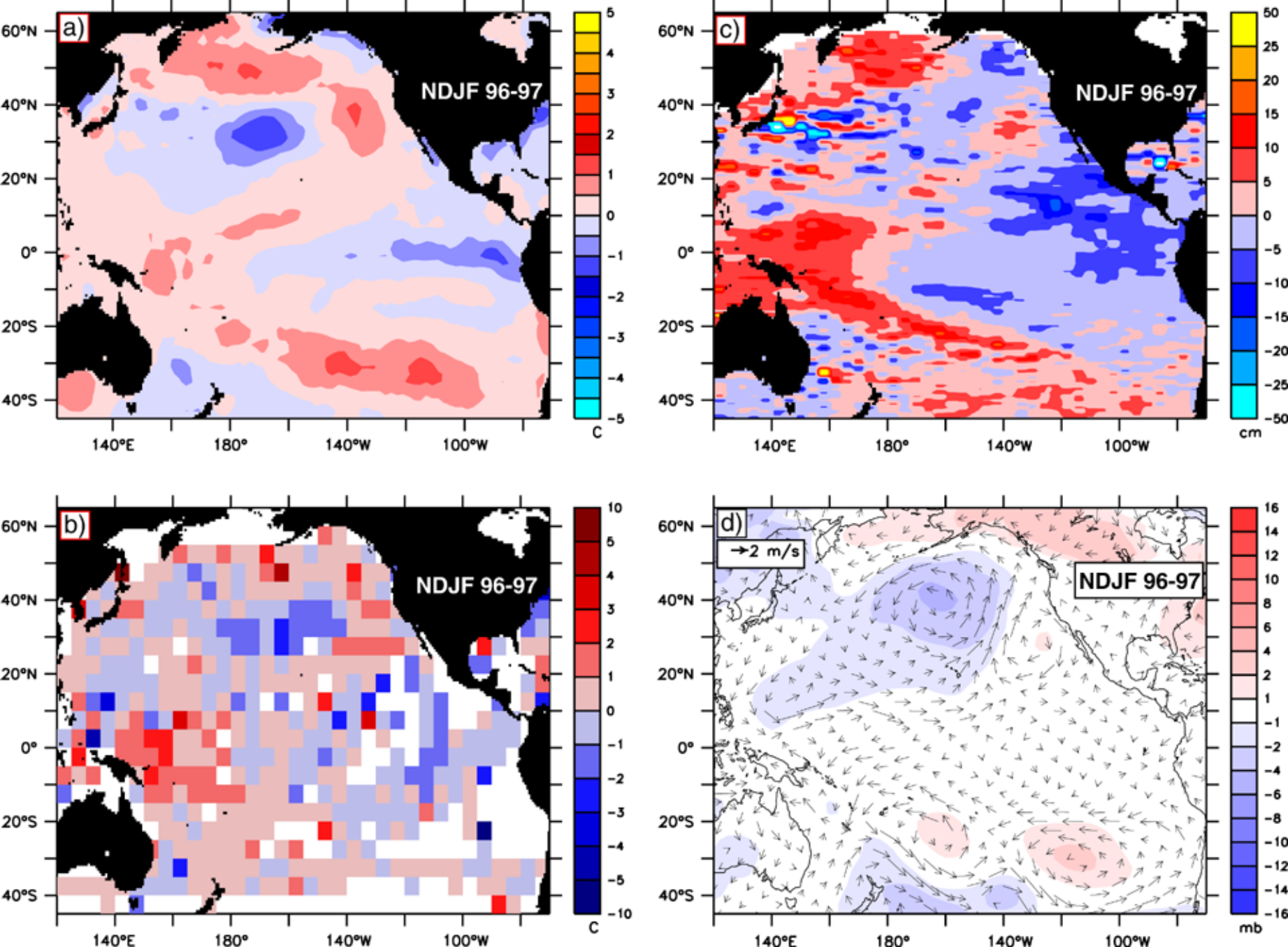
a)
NDJF 96-97
5
4
3
2
1
0
−1
−2
−3
−4
−5
C
c)
NDJF 96-97
50
25
20
15
10
5
0
−5
−10
−15
−20
−25
−50
cm
b)
NDJF 96-97
10
5
4
3
2
1
0
−1
−2
−3
−4
−5
−10
C
d)
→2 m/s
NDJF 96-97
16
14
12
10
8
6
4
2
1
−1
−2
−4
−6
−8
−10
−12
−14
−16
mb
60°N
40°N
20°N
0°
20°S
40°S
140°E
180°
140°W
100°W

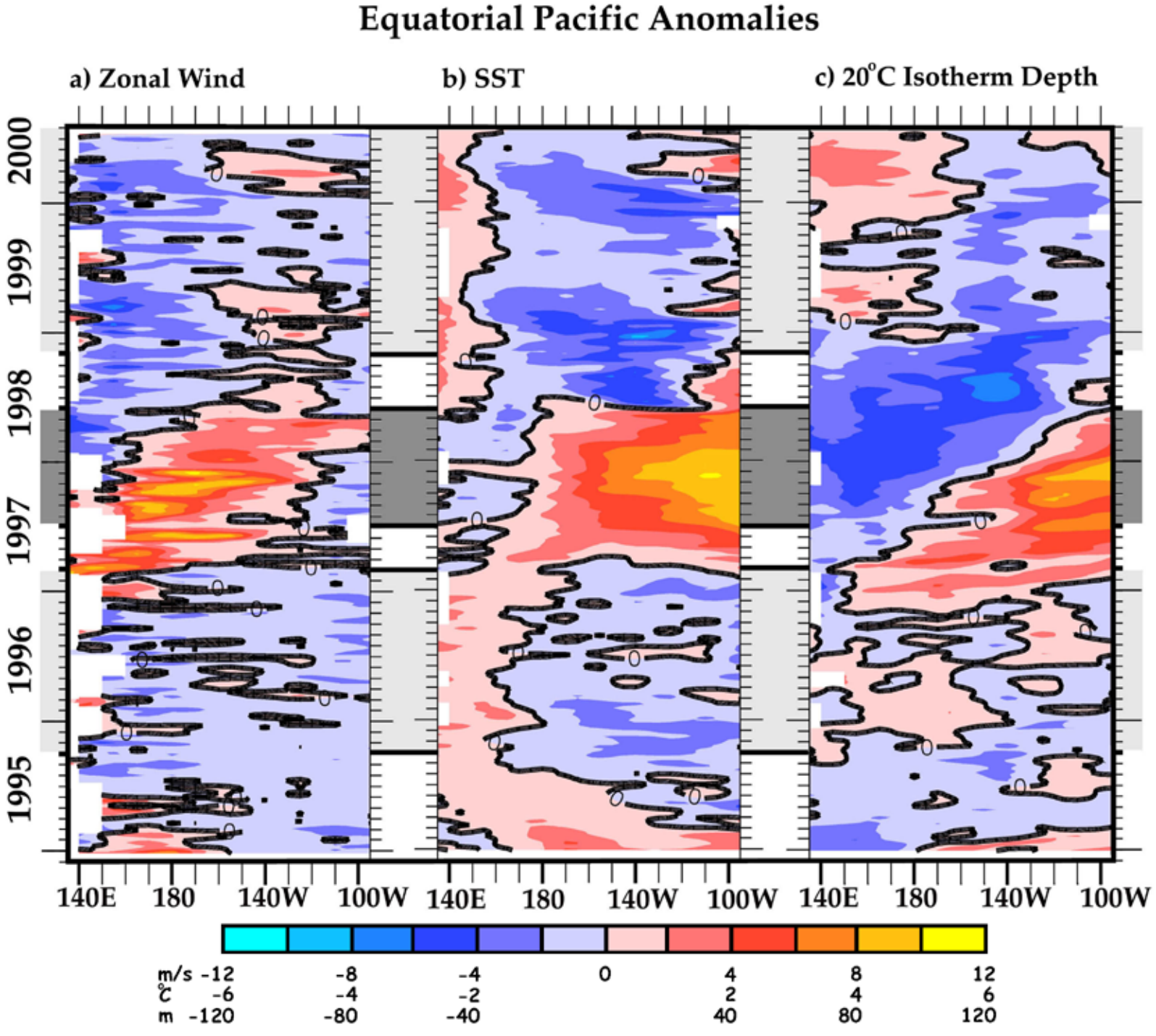
Equatorial Pacific Anomalies
a) Zonal Wind
b) SST
c) 20°C Isotherm Depth
2000
1999
1998
1997
1996
1995
140E
180
140W
100W
m/s -12 -8 -4 0 4 8 12
°C -6 -4 -2 2 4 6
m -120 -80 -40 40 80 120

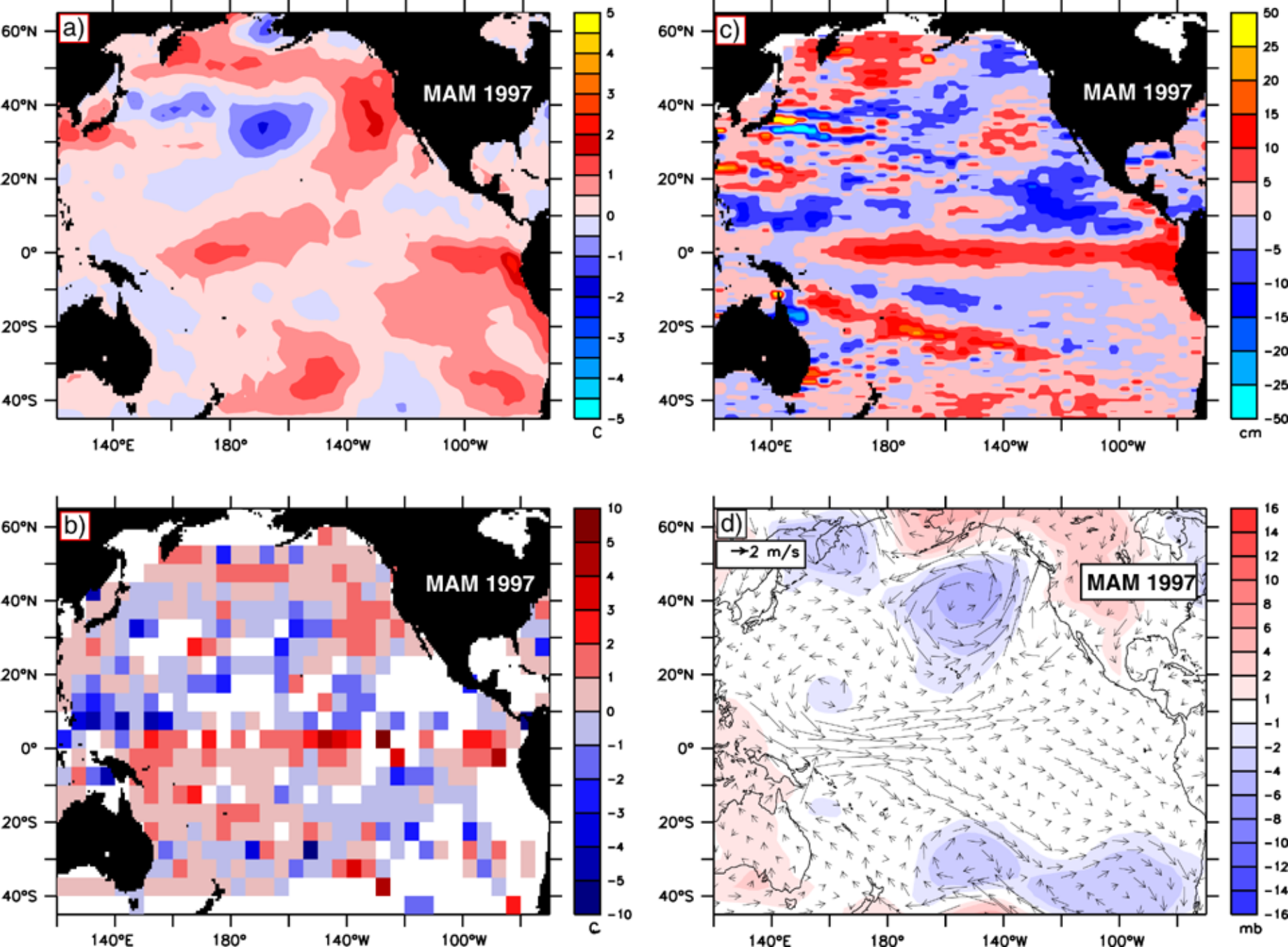
a)
MAM 1997
60°N
40°N
20°N
0°
20°S
40°S
140°E
180°
140°W
100°W
5
4
3
2
1
0
−1
−2
−3
−4
−5
C
c)
MAM 1997
50
25
20
15
10
5
0
−5
−10
−15
−20
−25
−50
cm
b)
MAM 1997
10
5
4
3
2
1
0
−1
−2
−3
−4
−5
−10
C
d)
→2 m/s
MAM 1997
16
14
12
10
8
6
4
2
1
−1
−2
−4
−6
−8
−10
−12
−14
−16
mb

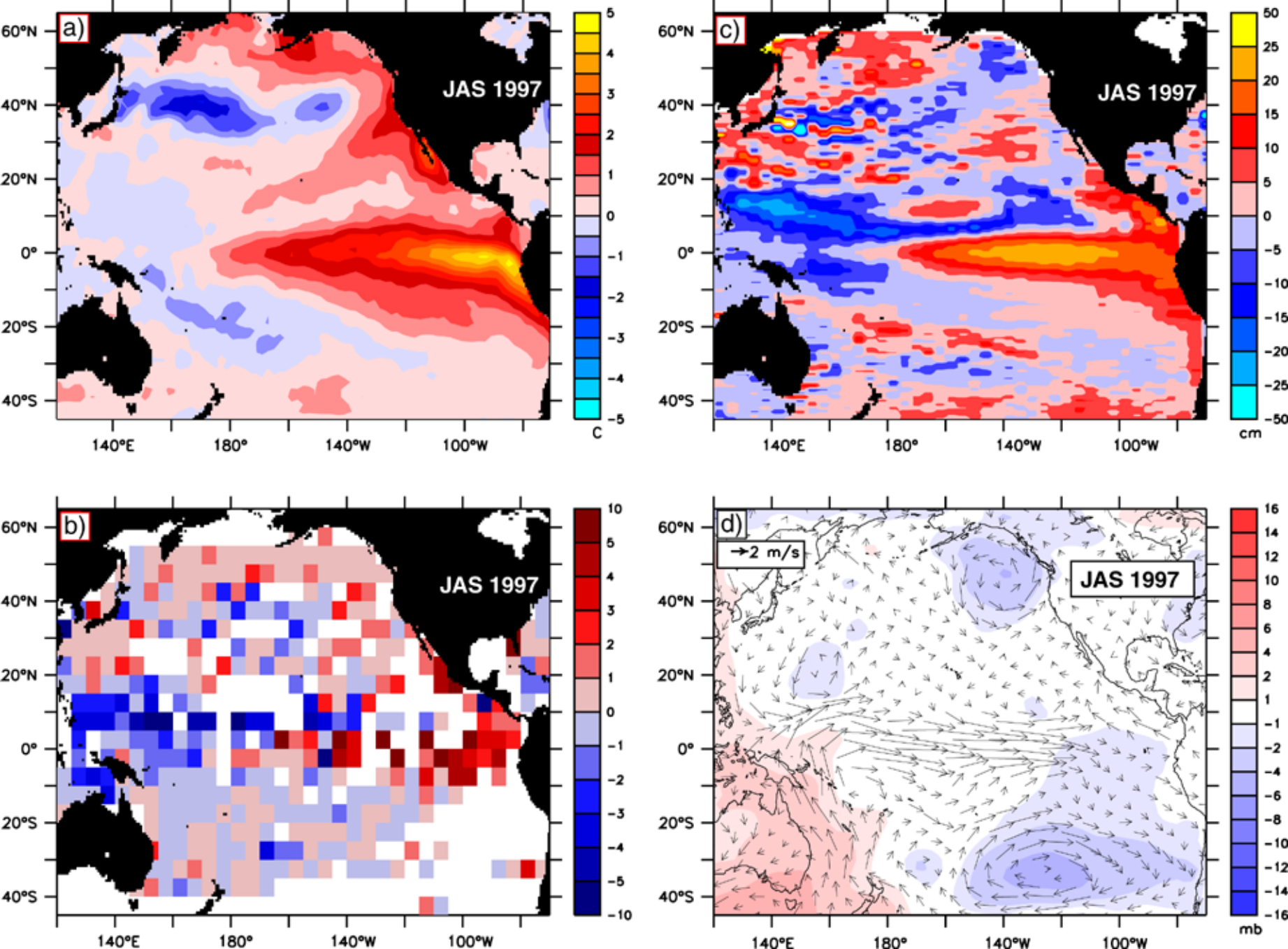
a)
JAS 1997
C
c)
JAS 1997
cm
b)
JAS 1997
d)
→2 m/s
JAS 1997
mb
60°N
40°N
20°N
0°
20°S
40°S
140°E
180°
140°W
100°W

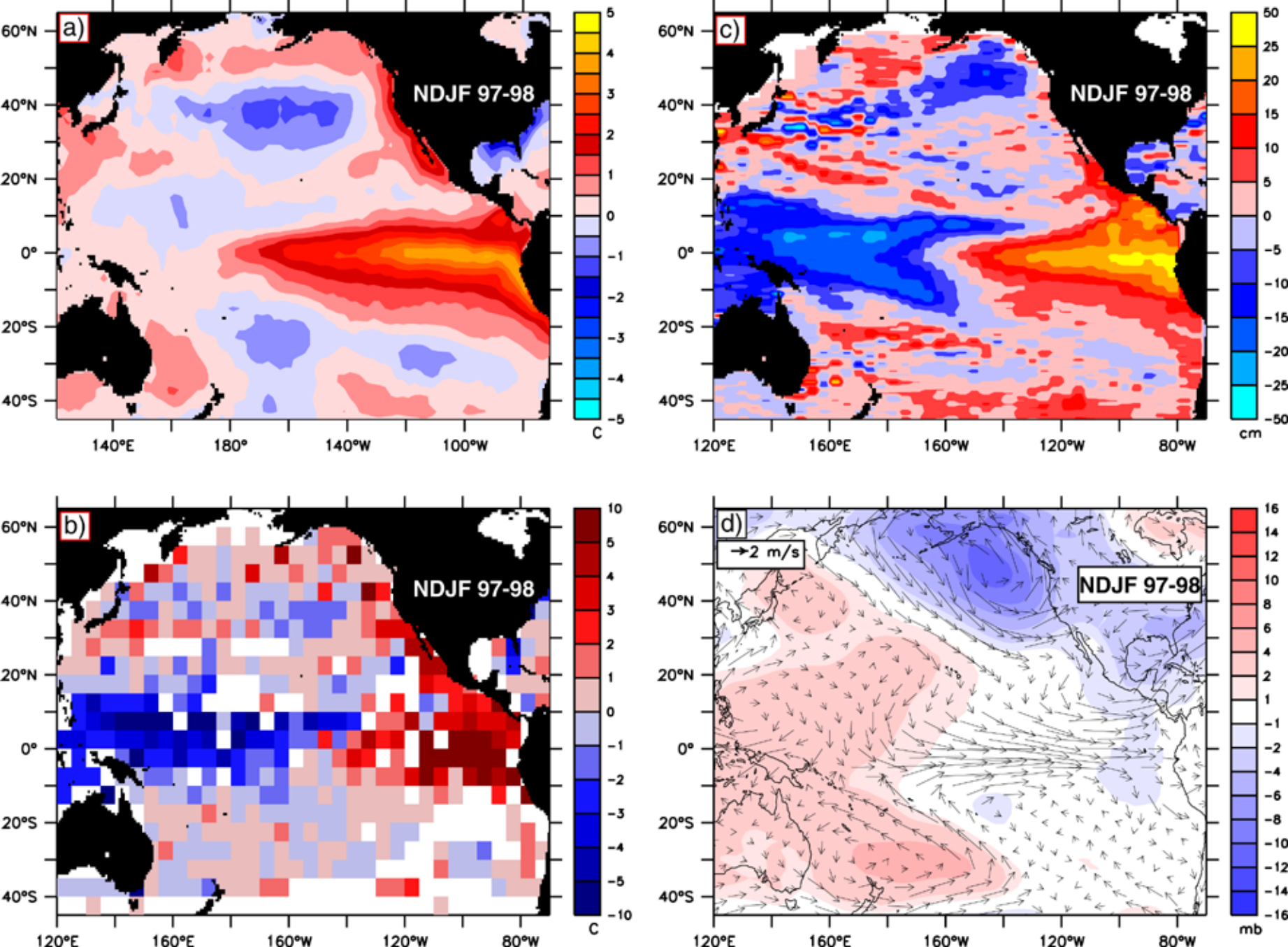
a)
NDJF 97-98
60°N
40°N
20°N
0°
20°S
40°S
140°E
180°
140°W
100°W
5
4
3
2
1
0
−1
−2
−3
−4
−5
C
c)
NDJF 97-98
120°E
160°E
160°W
120°W
80°W
50
25
20
15
10
5
0
−5
−10
−15
−20
−25
−50
cm
b)
NDJF 97-98
10
5
4
3
2
1
0
−1
−2
−3
−4
−5
−10
C
d)
→2 m/s
NDJF 97-98
16
14
12
10
8
6
4
2
1
−1
−2
−4
−6
−8
−10
−12
−14
−16
mb

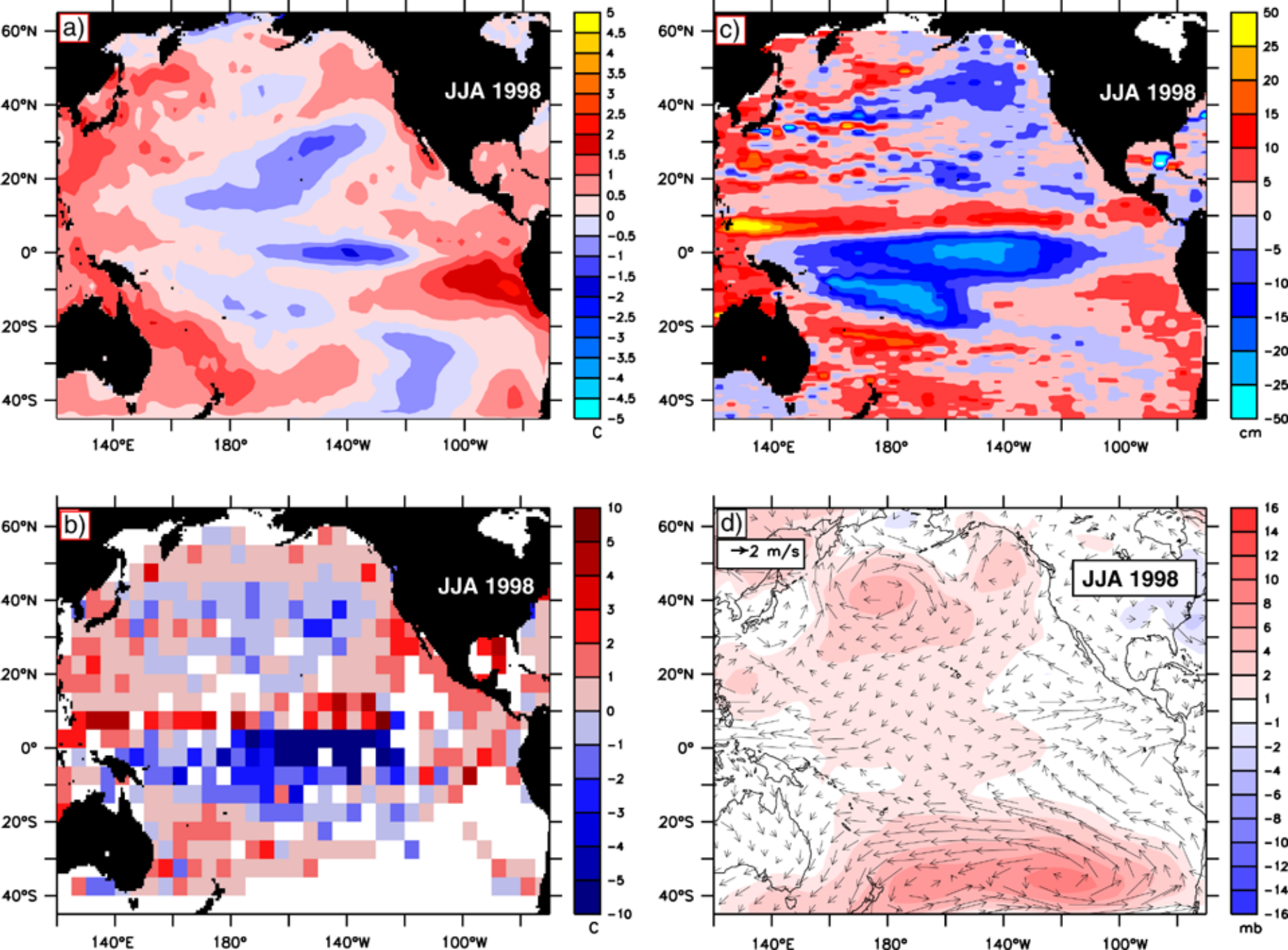
a)
JJA 1998
5
4.5
4
3.5
3
2.5
2
1.5
1
0.5
0
−0.5
−1
−1.5
−2
−2.5
−3
−3.5
−4
−4.5
−5
C
60°N
40°N
20°N
0°
20°S
40°S
140°E
180°
140°W
100°W
c)
JJA 1998
50
25
20
15
10
5
0
−5
−10
−15
−20
−25
−50
cm
b)
JJA 1998
10
5
4
3
2
1
0
−1
−2
−3
−4
−5
−10
C
d)
→2 m/s
JJA 1998
16
14
12
10
8
6
4
2
1
−1
−2
−4
−6
−8
−10
−12
−14
−16
mb

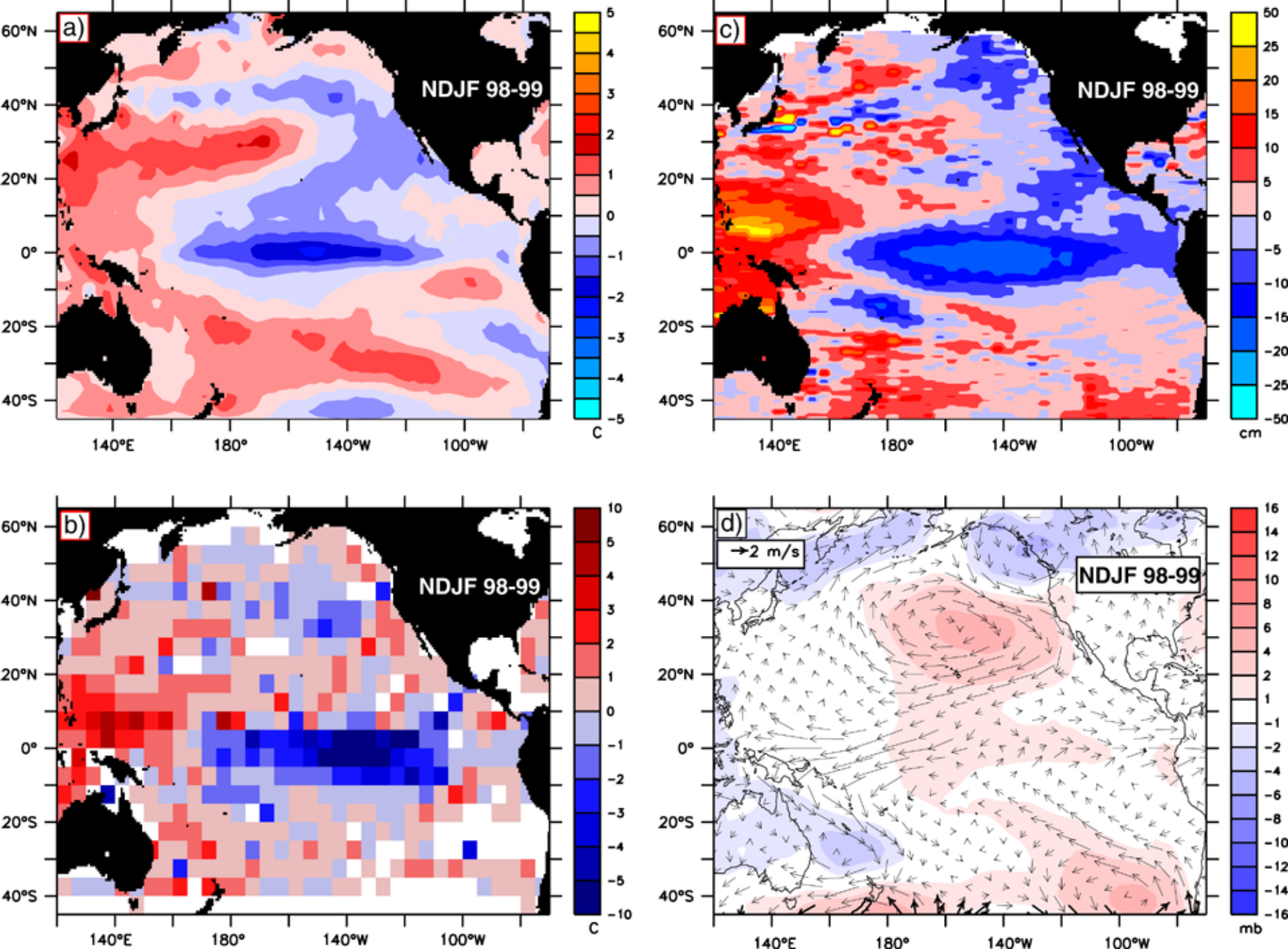
a)
NDJF 98-99
60°N
40°N
20°N
0°
20°S
40°S
140°E
180°
140°W
100°W
5
4
3
2
1
0
−1
−2
−3
−4
−5
C
c)
NDJF 98-99
50
25
20
15
10
5
0
−5
−10
−15
−20
−25
−50
cm
b)
NDJF 98-99
10
5
4
3
2
1
0
−1
−2
−3
−4
−5
−10
C
d)
→2 m/s
NDJF 98-99
16
14
12
10
8
6
4
2
1
−1
−2
−4
−6
−8
−10
−12
−14
−16
mb

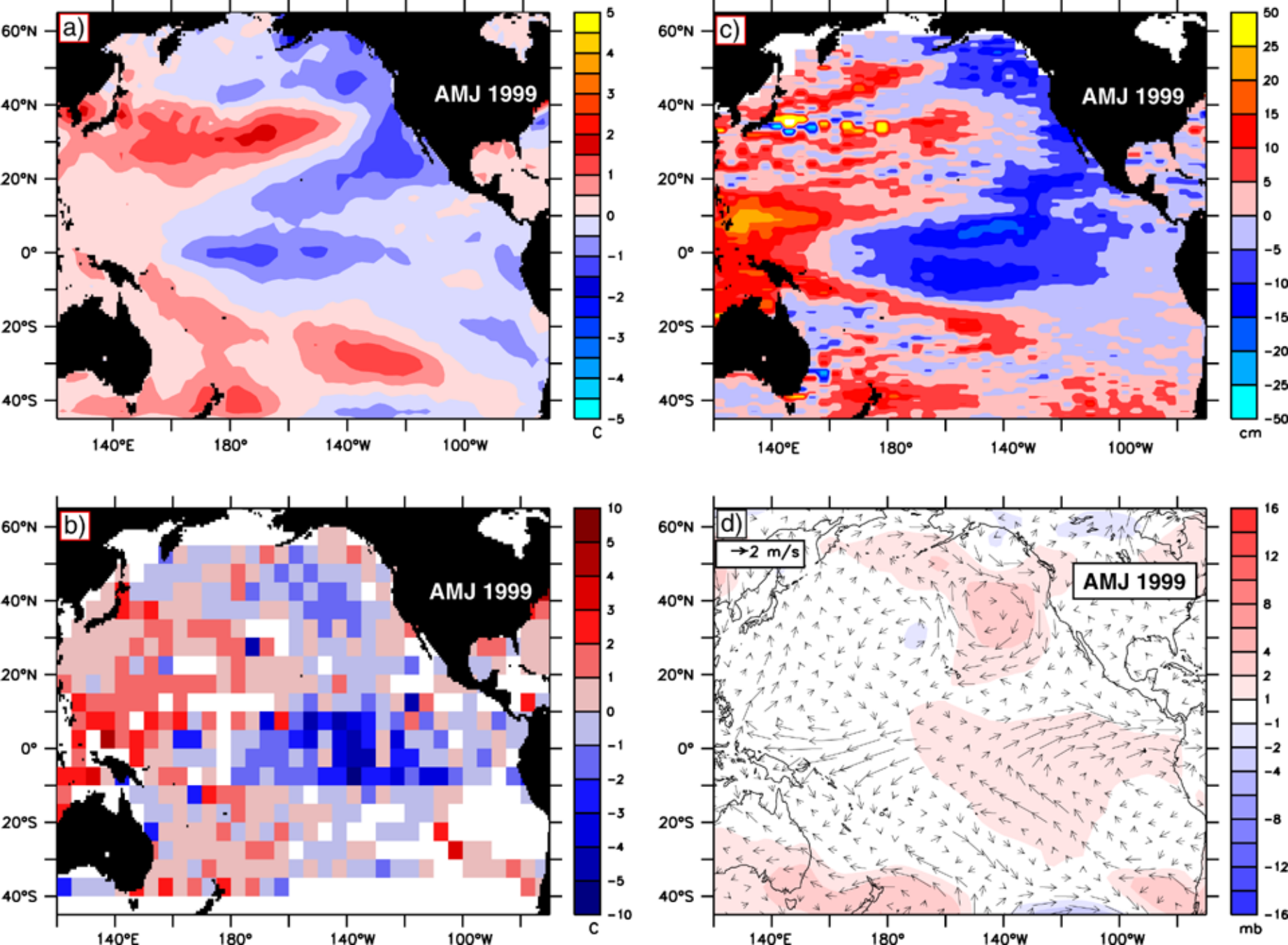
a)
AMJ 1999
60°N
40°N
20°N
0°
20°S
40°S
140°E
180°
140°W
100°W
5
4
3
2
1
0
−1
−2
−3
−4
−5
C
c)
AMJ 1999
50
25
20
15
10
5
0
−5
−10
−15
−20
−25
−50
cm
b)
AMJ 1999
10
5
4
3
2
1
0
−1
−2
−3
−4
−5
−10
C
d)
→2 m/s
AMJ 1999
16
12
8
4
2
1
−1
−2
−4
−8
−12
−16
mb

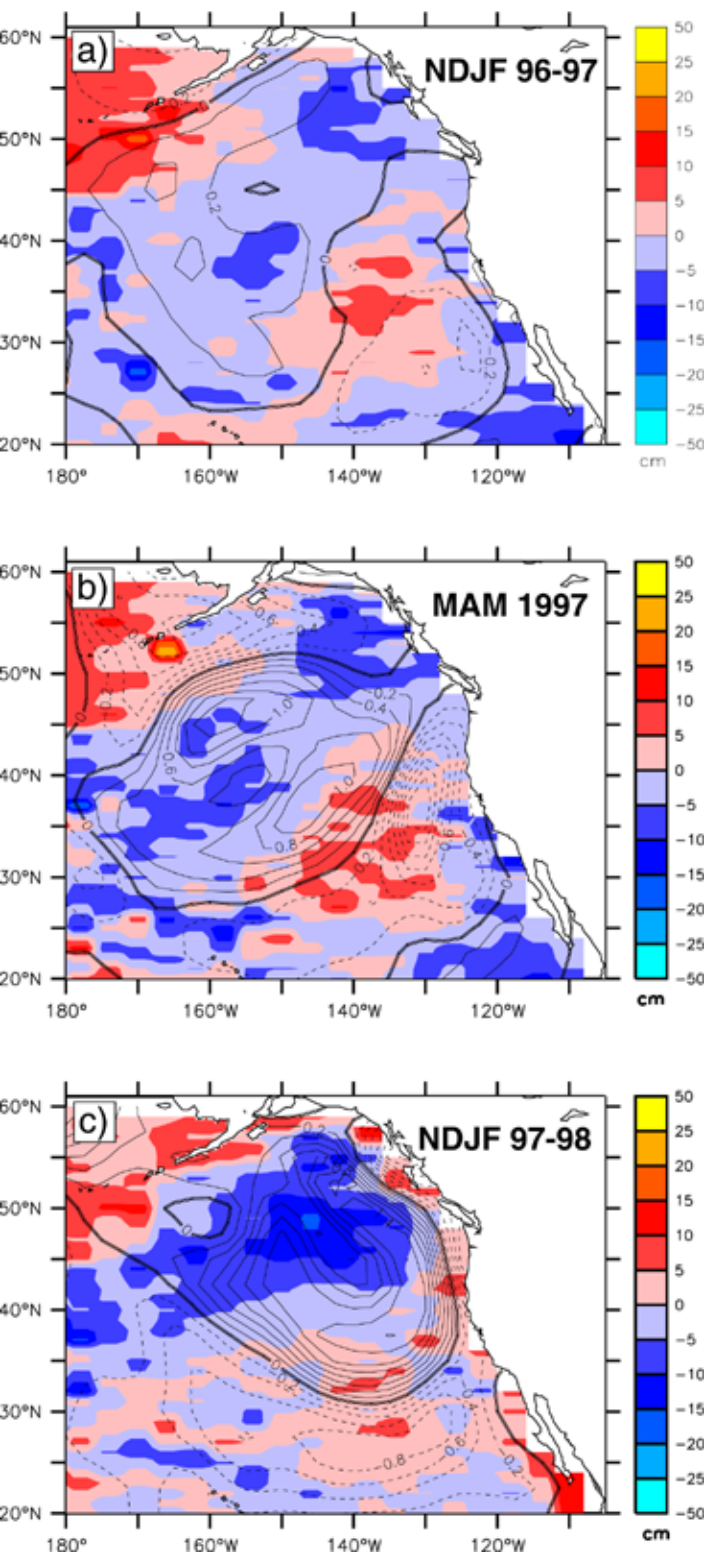
a)
NDJF 96-97
b)
MAM 1997
c)
NDJF 97-98
60°N
50°N
40°N
30°N
20°N
180°
160°W
140°W
120°W
50
25
20
15
10
5
0
−5
−10
−15
−20
−25
−50
cm